Renoguanylin stimulates apical CFTR translocation and decreases HCO_3-secretion through PKA activity in the Gulf toadfish (Opsanus beta)

DOI:
10.1242/jeb.173948

Renoguanylin stimulates apical CFTR translocation and decreases HCO_3^- secretion through PKA activity in the Gulf toadfish (*Opsanus beta*)

Ilan M. Ruhr*[,1], Kevin L. Schauer[1], Yoshio Takei[2], Martin Grosell[1]

Department of Marine Biology and Ecology, The Rosenstiel School of Marine and Atmospheric Science, The University of Miami, Miami, Florida, USA[1], Department of Marine Bioscience, The Atmosphere and Ocean Research Institute, The University of Tokyo, Kashiwa, Chiba, Japan[2]

Running Head: RGN regulates CFTR and PKA in *O. beta*

Keywords: PKG, Cl^- secretion, guanylin peptides, intestine, seawater teleost

*Corresponding Author

Current Institution: University of Manchester, Faculty of Biology, Medicine, and Health, Cardiovascular Sciences

Email: ilan.ruhr@manchester.ac.uk

Phone: 305.421.4665

Fax: 305.421.4600

Summary statement: RGN stimulation radically alters the physiology of Gulf toadfish enterocytes via PKA, by reversing ion-absorbing mechanisms, inhibiting HCO_3^- secretion, and causing insertion of CFTR into the apical membrane.

Abstract

The guanylin peptides – guanylin, uroguanylin, and renoguanylin (RGN) – are endogenously produced hormones in teleost fish enterocytes that are activators of guanylyl cyclase-C (GC-C) and are potent modulators of intestinal physiology, particularly in seawater teleosts. Most notably, they reverse normal net ion-absorbing mechanisms that are vital to water absorption, an important process for seawater teleost survival. The role of guanylin-peptide stimulation of the intestine remains unclear, but it is hypothesized to facilitate the removal of solids from the intestine by providing fluid to enable their removal by peristalsis. The present study uses one member of these peptides – RGN – to provide evidence for the prominent role that protein kinase A (PKA) plays in mediating the effects of guanylin-peptide stimulation in the posterior intestine of the Gulf toadfish (*Opsanus beta*). Protein kinase G is shown to not mediate the intracellular effects of RGN, despite previous evidence showing that GC-C activation leads to higher cyclic guanosine monophosphate formation. RGN is shown to reverse the absorptive short-circuit current and increase conductance in the Gulf toadfish intestine. These effects are correlated to increased trafficking of the cystic fibrosis transmembrane conductance regulator (CFTR) Cl^- channel to the apical membrane, which are negated by PKA inhibition. Moreover, RGN decreases HCO_3^- secretion, likely by limiting the exchange activity of SLC26a6 (a HCO_3^-/Cl^- antiporter), a reduction that is enhanced by PKA inhibition. RGN seems to alter PKA activity in the posterior intestine to recruit CFTR to the apical membrane and reduce HCO_3^- secretion.

Introduction

Seawater presents a major osmoregulatory challenge for teleost fish, due to the direct interaction of their thin respiratory epithelia – the gills – with the environment that causes unavoidable branchial fluid loss (Evans *et al.*, 2005). To compensate, the seawater teleost constantly drinks water and absorbs it across the intestine. Imbibed seawater undergoes rapid desalination by the esophagus, so, by the time it enters the intestine, its osmolality is roughly that of blood plasma. In the intestine, precipitation of Ca^{2+} and Mg^{2+} by HCO_3^- to form Ca- and $MgCO_3$ precipitates and titration of HCO_3^- by H^+ facilitate further decreases in intestinal fluid osmolality by up 130 mOsmol/kg (Grosell *et al.*, 2009a; Grosell *et al.*, 2009b; Wilson *et al.*, 2002). The combined effect of these processes, in addition to other ion-absorbing pathways, renders the fluid osmolality in the intestine similar to that of the extracellular fluids and allows for efficient water absorption that is coupled to Na^+ and Cl^- absorption (Skadhauge, 1969; Skadhauge, 1974). Even though net water absorption and the mechanisms that facilitate it are vital to the survival of teleosts living in seawater, recent studies reveal region-specific areas of the intestine that display net secretory functions, at least periodically (Ruhr *et al.*, 2014; Ruhr *et al.*, 2016).

In the Gulf toadfish (*Opsanus beta*), members of the homologous guanylin family of intestinal peptides [guanylin, uroguanylin, and renoguanylin (RGN)] reverse ion absorption in the posterior intestine, but not in the anterior region (Ruhr *et al.*, 2014). This reversal also corresponds to RGN-stimulated water secretion in the posterior intestine and rectum, but not in the anterior intestine (Ruhr *et al.*, 2014; Ruhr *et al.*, 2016). The switch from net ion absorption to net ion secretion (from mucosa-to-serosa to serosa-to-mucosa) seems to be caused primarily by inhibition of absorption by NKCC2 and HCO_3^-/Cl^- exchange activity and Cl^- secretion through the apical cystic fibrosis transmembrane conductance regulator (CFTR) channel (Ruhr *et al.*, 2014; Ruhr *et al.*, 2015; Ruhr *et al.*, 2016). This response is also isolated to the mid and posterior intestine of the Japanese eel (*Anguilla japonica*) after stimulation by guanylin (Ando, and Takei, 2015; Ando *et al.*, 2014; Yuge, and Takei, 2007). It is hypothesized that the inhibition of fluid absorption is required to facilitate the removal of solids, such as undigested food, fecal matter, or carbonate precipitates. The presence of fluid has been shown to enhance

70 the efficiency of peristalsis in mammals, thus, making the movement of solids through the intestinal tract
71 easier (Schulze, 2015).
72 A handful studies on the intestinal physiology of seawater teleosts have demonstrated a reversal
73 of ion absorption. In the winter flounder (*Pseudopleuronectes americanus*) intestine, atrial natriuretic
74 factor, vasoactive intestinal peptide (VIP), cyclic guanosine monophosphate (cGMP), and cyclic
75 adenosine monophosphate (cAMP) can alter NKCC2 activity and decrease the absorptive short-circuit
76 current (I_{SC}), which is a measure of total ion movement (O'Grady S, 1989; O'Grady *et al.*, 1988; O'Grady
77 *et al.*, 1985; Rao, and Nash, 1988; Rao *et al.*, 1984). These early studies demonstrate that the reversal of
78 net ion absorption in seawater teleosts is largely driven by Cl^- secretion, in addition to decreased activity
79 of absorptive-type ion transporters (O'Grady, and Wolters, 1990). A more recent study on the killifish
80 (*Fundulus heteroclitus*) similarly reveals that a combination of ionomycin, db-cAMP, and IBMX (a
81 phosphodiesterase inhibitor) stimulate fluid secretion in the posterior intestine (Marshall *et al.*, 2002). It is
82 interesting that intestinal tissues from multiple species of seawater teleosts respond to the above-
83 mentioned hormones, activators, and inhibitors by decreasing ion-absorbing mechanisms that, in some
84 cases, result in fluid secretion. The inhibition of ion transport and water absorption is widespread across
85 seawater teleost species and might serve a beneficial purpose for life in seawater. In both mammalian and
86 fish enterocytes, stimulation of the apical guanylin peptide receptor, guanylyl cyclase-C (GC-C), leads to
87 increased formation of cGMP (Chao *et al.*, 1994; Kuhn *et al.*, 1994; Schulz *et al.*, 1990; Yuge, and Takei,
88 2007) that activates protein kinase G (PKG) and increases cAMP formation (leading to PKA activation)
89 (Arshad, and Visweswariah, 2012; Arshad, and Visweswariah, 2013). Stimulation of GC-C leads to
90 apical CFTR activation, inhibition of Na^+/H^+-exchangers (NHEs) in mammals, inhibition of NKCC2 in
91 fish, and decreases HCO_3^- secretion in fish (Chao *et al.*, 1994; Ruhr *et al.*, 2014; Ruhr *et al.*, 2016).
92 In the present study, we investigated the intracellular effects of RGN in Gulf toadfish enterocytes.
93 Our first goal was to determine if RGN affected CFTR abundance in the apical membrane. We have
94 previously shown that CFTR is likely present in the posterior intestine of the Gulf toadfish, but that it is
95 mostly sub-apical. We hypothesize that RGN stimulation will increase insertion of CFTR into the apical

membrane. The present study corroborates these findings by measuring the I_{SC} and transepithelial conductance (G_{TE}) of the tissues. Our second goal was to see whether the RGN response was mediated primarily by PKG or PKA. We hypothesize that PKA plays a greater role in mediating the RGN response, based partly on the fact that cAMP/PKA are involved in trafficking CFTR in the rat jejunum and in *Xenopus laevis* oocytes (Golin-Bisello *et al.*, 2005; Weber *et al.*, 1999).

Materials and Methods

Experimental animals

Gulf toadfish were caught as bycatch from Biscayne Bay, FL. Upon arrival in the laboratory, ectoparasites were removed by a 3-min freshwater bath and treatment with malachite green in seawater. Fish were separated by size/weight classes and placed into 62-litre aerated tanks (33-36 ppt, 20-26°C), with continuous flow-through of sand-filtered SW from Biscayne Bay. Fish were fed weekly to satiation with squid, but fasted for at least three days prior to experimentation. Fish husbandry and experimental procedures were in accordance with the University of Miami Animal Care Protocol (IACUC no. 13-225, renewal 03, and 15-019, renewal 02). MS-222 (0.2 g l^{-1}; Argent, Redmond, WA, USA) solution buffered with 0.3 g l^{-1} $NaHCO_3^-$ (Sigma-Aldrich, St. Louis, MO, USA) was used to anaesthetize fish prior to sacrificing them by severing the spinal cord at the cervical vertebra and pithing of the brain.

Composition of salines, hormones, activators, and inhibitors

Mucosal (pH = 7.8) and serosal (pH = 7.8) salines were prepared as described in (Table 1) and used to bathe intestinal tissues. Eel RGN (Peptide Institute, Ibaraki-Shi, Osaka, Japan) was used in the present study as the activator and a tool to assess the function of activating GC-C in the posterior intestine. The purity of biologically active eel RGN was confirmed using reversed-phase, high-performance liquid chromatography (Yuge, and Takei, 2007). The amino acid sequence of eel RGN (ADLCEICAFAACTGCL, accession number: BAC76010.1) is nearly identical to Gulf toadfish guanylin (MDVCEICAFAACTGC, accession number: AIA09902.1) and stimulation of the Gulf toadfish posterior intestine with eel RGN has the greatest physiological effects compared to eel uroguanylin or eel guanylin (Ruhr *et al.*, 2014).

Activators and inhibitors were dissolved in either water, dimethylsulphoxide (DMSO; Sigma-Aldrich), or ethanol (EtOH; Sigma-Aldrich). The PKG inhibitors, KT5823 and Rp-8-pCPT-cGMPS (Enzo Life Sciences, Farmingdale, NY, USA), were dissolved in DMSO and water, respectively. The cGMP analog/PKG activator, 8-Bromo-cGMP (Enzo), was dissolved in water. The PKA inhibitors, H-89

(dihydrochloride; Cell Signalling Technologies, Beverly, MA, USA) and PKI (14-22, amide, myristoylated; Enzo)were dissolved in DMSO. Final concentrations: KT5823 (2 μmol l^{-1}), Rp-8-pCPT-cGMPS (25 μmol l^{-1}), 8-Bromo-cGMP (100 μmol l^{-1}), H-89 (20 μmol l^{-1}), and PKI 10 μmol l^{-1}). The concentrations for these inhibitors were tested using the recommended dose by their respective manufacturers (and no surpassing the solubility that would excede the ideal DMSO or EtOH content in the saline). Final solvent ratios in which inhibitors were dissolved 1:1000 (0.1%) and 1:2000 (0.05%) for DMSO and EtOH, respectively. Vehicle controls for 0.1% DMSO and 0.05% EtOH did not affect the physiological parameters tested in the present (data not shown) and previous studies on Gulf toadfish (Ruhr *et al.*, 2014; Ruhr *et al.*, 2015; Ruhr *et al.*, 2016).

General experimental protocol: short-circuit current and pH-stat titration

I_{SC}, *TEP*, and G_{TE} of Gulf toadfish tissues were measured by Ussing chambers (model 2400; Physiologic Instruments). The posterior intestine of a Gulf toadfish (15-30 g) was excised, cut open along the midline, mounted onto P2413 tissue holders (Physiologic Instruments) to expose 0.71 cm^2 of tissue, and placed between the two half-chambers of the Ussing apparatus. I_{SC} and *TEP* were measured by silver (Ag) current and Ag/AgCl voltage electrodes, respectively, and were connected to an amplifier (model VCC600, Physiologic Instruments, San Diego, CA, USA). I_{SC} was measured using current electrodes under voltage-clamp conditions (0.0 mV), with 3 s of 2-mV pulses (mucosal-to-serosal) every 60 s. *TEP* was measured by voltage electrodes under current-clamp conditions (0.0 μA), with 3 s of 30-μA pulses (mucosal-to-serosal) every 60 s. G_{TE} was calculated by Ohm's law and was determined from the deflections in I_{SC} and *TEP* during pulsing. Acqknowledge software (v. 3.8.1, BIOPAC Systems, Goleta, CA, USA) recorded I_{SC} and *TEP* onto a computer. The function and viability of Gulf toadfish intestinal tissues are stable in the Ussing chamber for more than 2 h (Ruhr *et al.*, 2014).

I_{SC} measurements were taken under symmetrical conditions using 2 ml of serosal saline (Table 1) in each half-chamber (the mucosal/apical/luminal and the serosal/basolateral/blood-side chambers). The salines were continually mixed by airlift gassing (0.3% CO_2/99.7% O_2) and maintained at 25 °C by a

recirculating bath (model 1160S, VWR, Radnor, PA USA), as described in Grosell and Genz (Grosell, and Genz, 2006).

TEP measurements were taken under asymmetrical conditions using 2 ml of mucosal and HCO_3^-/CO_2-free serosal saline (Table 1), which were added to their respective half-chambers. A previous study on the Gulf toadfish revealed that RGN might regulate the transport activity of SLC26a6 (Ruhr *et al.*, 2016). This previous study used an HCO_3^-/CO_2-free serosal saline to render the basolateral NBCe (a Na^+/HCO_3^--cotransporter) functionless and determined that the effects of RGN decreased the transport activity of SLC26a6, independent of cytosolic carbonic anhydrase activity. Accordingly, the present study also used a HCO_3^-/CO_2-free serosal saline to investigate the role of PKA and PKG activators and stimulants on SLC26a6 activity. The mucosal saline was continually mixed by airlift gassing (100% O_2) and the serosal saline as described above and maintained at 25°C. HCO_3^- secretion was measured using a pH-stat titrator (model TIM 854 or 856, Radiometer, Loveland, CO, USA) that was set up in tandem with an Ussing chamber system [described by Grosell and Genz (Grosell, and Genz, 2006)]. The mucosal pH of 7.8 was maintained using a pH electrode (Radiometer, model PHC4000.8) and an acid-delivering microburette tip (0.005 N HCl); both were immersed in the mucosal saline bath, allowing for symmetrical pH conditions on either side of the epithelium. The volume of acid titrant and mucosal pH were measured and recorded using Titramaster software (Radiometer, v. 5.1.0) onto a computer. The HCO_3^- secretion rate from a tissue preparation was calculated from the rate of titrant secreted and its concentration [described by Grosell and Genz (Grosell, and Genz, 2006)]. RGN was added to the mucosal half-chamber, using a concentration of 10^{-7} mol l^{-1}.

Intestinal sac preparations and immunohistochemistry

Sac preparations from the posterior intestine were made and preserved for immunohistochemistry to determine the effects of RGN on CFTR translocation. The posterior intestine (1.5-3 cm) from Gulf toadfish (50-80 g) was excised as described above. Briefly, following a modified protocol (Ruhr *et al.*, 2016), the flared end of a PE50 catheter was inserted into the posterior intestine and tied off with a silk

suture. Mucosal saline (Table 1) was then injected into the catheter to rinse the tissue of any debris. The open end of the tissue was then tied off with silk suture to form an intestinal sac. The sac preparations were then injected with mucosal saline (control or containing 5×10^{-7} mol l^{-1} RGN). The catheter was sealed and placed in a scintillation vial containing serosal saline and continually gassed with 0.3% CO_2 (Table 1) for 1 h. At the end of the experimental period, the sac preparations were removed from the serosal saline. After the silk sutures were cut and the catheter removed, the tissue was drained and placed into Z-fix (Anatech, Hayward, CA, USA) for 48 h to fix the tissue. Following fixation, the tissue was immersed in 70% ethanol for 1 week. Then, ascending grades of ethanol washes (3x in 95%, followed by 3x in 100%) were used to dehydrate tissues. Tissues were then prepared for wax embedding by immersion in butanol, two washes in Histochoice (Amresco, Solon, OH, USA), and four washes in paraplast (McCormick Scientific, St. Louis, MO, USA), after which tissues were embedded in Luckart bars. A microtome (model 1512, Leitz, Grand Rapids, MI, USA) was used to slice sections of tissue (4 μm); the tissue sections from the posterior intestine and rectum were mounted onto poly-L-lysin-coated slides and dried for 24 h at 37°C.

Tissues were prepared for antibody treatment by immersing slides into two washes of Histochoice (to remove the paraplast), followed by descending grades of ethanol (100%, 2 x 90%, 70%, and 50%) and 2 washes in phosphate-buffered saline (PBS) (pH 7.3). To reveal antigenic sites, the following steps were taken. Slides were first incubated in 10 mmol l^{-1} of citric acid solution (pH 6) and heated to boiling in a microwave for two 5-min incubations at 80% power. Next, slides were cooled to room temperature and were washed in the following order: 0.05% sodium dodecyl sulfate (SDS)-PBS for 5 min, solution A [PBS, NaCl (58.44 mmol l^{-1}), 0.2% Tween-20 (Sigma-Aldrich), and pH 7.3] for 5 min, and Image-iT (Life Technologies) for 30 min. To block non-specific antigenic sites, slides were incubated for 1 h in PBS solution containing 5% skim milk, 1% bovine serum albumin (BSA), and 0.05% Tween-20. Slides were rinsed twice in PBS after each step.

Tissue sections from the posterior intestine and rectum were probed with fluorescent antibodies. The primary monoclonal mouse CFTR antibody [Human CFTR C-Terminus MAb (Clone 24-1), Mouse

IgG2A, Cat #: MAB25031, R&D Systems] was diluted to 10 μg ml^{-1} in PBS solution containing 0.5% skim milk, 1% BSA, and 0.05% Tween-20. This particular CFTR antibody was used previously by our group to reveal CFTR localization in the intestine of the Gulf toadfish (Ruhr *et al.*, 2014)] and has been validated using Western blot analysis in the Gulf toadfish gill with an approximate mass of 135 kDa (unpublished data). A hydrophobic pen was used to create a border around the tissues on a slide, inside of which primary antibody was deposited. Slides were placed in a humid chamber on an oscillating table at 5°C overnight, then rinsed twice in PBS containing 0.05% Tween-20 and once in normal PBS. The following steps occurred in the absence of light. Donkey anti-mouse IgG secondary antibody (Alexa Fluor 488, Cat #: AB_2556542, Thermo Fisher Scientific, Waltham, MA, USA) was diluted to 10 μg $m l^{-1}$ in PBS solution containing 0.5% skim milk, 1% BSA, and 0.05% Tween-20. The anti-mouse IgG was deposited inside the hydrophobic border surrounding the tissues. Slides were incubated in a humid chamber for 1 h at 37°C, after which they were rinsed twice in PBS containing 0.05% Tween-20 and once in normal PBS. ProLong Gold Antifade Reagent (Thermo Fisher Scientific) was used to adhere coverslips onto each slide.

Control slides were treated the same as above, with the exception of primary antibody treatment. Slides were observed with an Olympus fluorescent microscope (u-tvo.5xc-2), and images were taken with an attached QImaging camera (Retiga EXi, Fast 1394) using 40x magnification. Fiji (Schindelin *et al.*, 2012), iVision, and Gimp software were used to analyze the images. Three slides were analyzed for each individual (n = 4 per treatment).

A modified procedure was used to determine corrected membrane fluorescence using ImageJ (Potapova *et al.*, 2011). Briefly, a region was drawn around the apical membrane region for CFTR (that excludes the subapical staining). Then the fluorescent intensity within a selected region was calculated. On the same slide, a measurement of an area without fluorescent objects was used as the background subtraction. To calculate the corrected fluorescence, the area of the selected tissue was multiplied by the background intensity, which was then subtracted from the intensity of the selected region. Corrected fluorescent values were expressed relative to the control tissues, which were given a value of 1.0.

Whole intestine, cytoplasm, and cell membrane isolation

Sections of the posterior intestine were mounted onto Ussing chambers, as described above for measuring I_{SC}, and treated with RGN, and H-89. The physiological data were used to correlate changes in CFTR trafficking to I_{SC} and G_{TE}. Samples were prepared for Western blot analysis following a modified protocol used previously in fish (Tresguerres *et al.*, 2007). Briefly, tissues were then snap frozen in liquid nitrogen and stored in -80°C. In order to achieve sufficient protein yield, tissues from each treatment were pooled in groups of three and were pulverized in a porcelain grinder and weighed, after which ice-cold homogenization buffer [250 mmol l^{-1} sucrose, 1 mmol l^{-1} EDTA, 1x HALT Protease Inhibitor Cocktail (Thermo Fisher Scientific) and 30 mmol l^{-1} Tris at pH 7.4] was added in a 1:10 w/v ratio. Samples were sonicated on ice for three 10-s pulses, and centrifuged (3000 g, 10 min at 4°C). The supernatant was collected; some were stored as the whole intestine sample and the rest was centrifuged once more (20,800 g, 30 min at 4°C). The supernatant was collected (the cytoplasmic fraction) and the pellet re-suspended in homogenization buffer (the membrane fraction). Following this, protein concentrations were determined via the bicinchonic acid method (Thermo Fisher Scientific), according to the manufacturer's instructions.

Western blot analysis

Samples were prepared in Laemmli sample buffer (Bio-Rad) at a concentration of 0.5-1.0 μg ml^{-1} for Western blot analysis. Proteins were separated on 4-15% SDS-PAGE gels (Bio-Rad) at 200V and transferred to polyvinylidene fluoride (PVDF) membranes via wet transfer for 60 min at 90V. The PVDF membrane was then blocked using Pierce™ Protein-Free (PBS) Blocking Buffer (Thermo Fisher Scientific) for 1 h and then incubated at 5°C overnight in primary mouse CFTR antibody (see immunohistochemistry) or with primary polyclonal rabbit Na^+/K^+-ATPase (NKA; Na^+/K^+-ATPase-α Antibody (H-300), Cat#: SC-28800, Santa Cruz Biotechnology, Dallas, TX, USA) to confirm the purity of each isolated fraction (membrane, cytoplasm, and whole intestine subsamples), diluted 1:150 and 1:200, respectively, with the blocking buffer containing 0.05% Tween-20 (Sigma-Aldrich). The primary

antibody was then discarded and blots were washed three times using tris-buffered saline containing 0.05% Tween-20 (TBS-T). Secondary antibody for CFTR (HRP-conjugated donkey anti-mouse IgG, Santa Cruz Biotechnology) and NKA (donkey anti-rabbit IgG-HRP, Cat#: SC-2313, Santa Cruz Biotechnology) diluted 1:1500 and 1:2000, respectively, with blocking buffer containing 0.05% Tween-20 was then added to the blots and incubated at room temperature for 1 h. Finally, blots were rinsed five times with TBS-T, developed using WesternSure ECL (Li-Cor, Lincoln, NE, USA), and imaged on a C-DiGit chemiluminescent scanner (Li-Cor). CFTR band intensity (~169 kDa) was determined using Image Studio Lite (Li-Cor). The control, RGN, and RGN + H-89 treatments were run concurrently on the same gel to ensure complete comparability. Upon completion of the western blotting, blots were stained with Coomassie Brilliant Blue, imaged on a personal scanner, and total protein was quantified using Image Studio Lite. Western blotting results were subsequently normalized to total protein in each lane to account for variations introduced during sample loading. Protein abundance was calculated relative to the appropriate control group.

Statistical analyses

The data are presented as means ± the standard error of the mean (SEM) and were evaluated using parametric and non-parametric statistical tests, as described in the figure legends. Means were considered significantly different with $P \leq 0.05$. Control measurements for I_{SC}, *TEP*, and HCO_3^- secretion were calculated from the final 30 min of the control fluxes and treatment values were calculated from the final 30 min of a 70-min treatment exposure. All p-values for the two-tailed Holm-Sidak tests are listed in Table 2.

Results

Membrane isolation and confirmation of CFTR band

NKA bands (105 kDa) are clearly visible in the membrane fraction, less so in the whole intestine fraction, and absent in the cytoplasmic samples (Fig. 1A). This confirms that the membrane isolation protocol was successful, as NKA is well known to be confined to the enterocyte basolateral membrane (Loretz, 1995) and, in the Atlantic salmon (*Salmo salar*) gill, has a molecular weight up 89-94 kDa (McCormick *et al.*, 2009). Subsequently, Western blots for CFTR were conducted and confirmed the presence of CFTR slightly greater than 150 kDa in the membrane fraction (Fig. 1B), in agreement with molecular weights of human CFTR that vary between 142-168 kDa (GenBank: AAA51980.1).

Stimulation by renoguanylin and inhibition of PKA and PKG

The absorptive I_{SC} of isolated posterior intestinal segments was reversed (from mucosa-to-serosa to serosa-to-mucosa) and G_{TE} increased by RGN stimulation (Fig. 2A, B). The effect of RGN was not affected by the addition of a PKG inhibitor (KT5823; n = 8, P = 0.642) (Fig. 2A, B).

The PKA inhibitor, H-89, partially, yet significantly, inhibited the effects of RGN on the absorptive I_{SC} and G_{TE} (Fig. 3A, B). H-89 also decreased the absorptive I_{SC}, which was fully reversed with the addition of RGN; furthermore, H-89 significantly decreased G_{TE}, which was then increased by RGN to a value that surpassed the control (Fig. 3C, D). There was no effect on I_{SC} and G_{TE} by vehicle dosages of DMSO [in which H-89 stocks were prepared (Fig. 3E, F)]. (All activators and inhibitors were added to the mucosal side of the tissue.)

Translocation of CFTR to the apical membrane

Western blots for CFTR reveal that RGN stimulation of posterior intestinal tissues increases the intensity of the CFTR band in the membrane fraction, while pre-treatment with H-89 eliminated changes in band intensity (Fig. 4). In addition, immunohistochemistry shows that CFTR fluorescence increases significantly in the apical membrane of RGN-treated tissues, when compared to control (Fig. 5).

306

307 *HCO_3^- secretion and transepithelial potential*

308 RGN stimulation alone reduces HCO_3^- secretion from 0.322 ± 0.038 to 0.260 ± 0.020 μmol cm^{-2}
309 h^{-1} in the posterior intestine, and further reduced to 0.206 ± 0.012 μmol cm^{-2} h^{-1} after the addition of H-89
310 (Fig. 6A). RGN also reverses the negative transepithelial potential (TEP), but has no effect on
311 transepithelial conductance (G_{TE}); the subsequent addition of H-89 partially reverses the effect on the TEP
312 by RGN and decreases G_{TE} (Fig. 6B). Comparatively, H-89, by itself, has no effect on HCO_3^- secretion
313 (0.284 ± 0.012 and 0.273 ± 0.022 μmol cm^{-2} h^{-1}, control and H-89 treatment, respectively), however, the
314 addition of RGN does reduce HCO_3^- secretion to 0.258 ± 0.025 μmol cm^{-2} h^{-1} (Fig. 6C). G_{TE} is reduced by
315 H-89 alone and the negative TEP is reversed by the combination of H-89 + RGN (Fig. 6D). A Student's t-
316 test reveals that baseline HCO_3^- secretion ($\Delta J_{HCO_3^-}$) is decreased more greatly by RGN alone (17.5 ±
317 3.9%) than by RGN being added -after H-89 (9.6 ± 3.3%) [Fig. 6A, C (P = 0.018)]. This indicates an
318 inhibitory effect of H-89 on RGN-induced responses.
319
320
321
322

Discussion

The present study confirms the presence of CFTR in the plasma membrane of the posterior intestine of the Gulf toadfish, by Western blot analysis and apical localization by immunohistochemistry. There is increased translocation of CFTR to the apical membrane after stimulation of the enterocytes with RGN that coincides with a reversal of the absorptive I_{SC} that is suppressed by PKA inhibition. RGN stimulation also leads to inhibited HCO_3^- secretion. The downstream effects of RGN stimulation seem to be primarily mediated by PKA, rather than PKG.

The downstream effects of RGN on PKA

Guanylin, uroguanylin, and RGN are endogenous activators of GC-C in vertebrates (Currie *et al.*, 1992; Greenberg *et al.*, 1997; Hamra *et al.*, 1993; Yuge, and Takei, 2007) and have been shown to regulate body electrolyte and fluid homeostasis by modulating the activity of various ion transporters (Arshad, and Visweswariah, 2012; Forte, 1999; Forte, and Hamra, 1996). In vertebrates, this occurs through elevated cGMP formation (Currie *et al.*, 1992; Iio *et al.*, 2005; Yuge *et al.*, 2006) that can increase PKG activity, modulate cAMP abundance, and regulate PKA activity (Arshad, and Visweswariah, 2013). The results of the present study on the Gulf toadfish suggest a greater role for PKA, rather than PKG, in the downstream pathways activated by RGN. Indeed, inhibition of PKA (by H-89) significantly reverses the effect of RGN on the absorptive I_{SC} and *TEP*, while inhibition of PKG does not. However, the inhibitory effect of PKA is partial and might be due the fact that (i) PKA is involved in more than one signalling pathway, (ii) H-89 will target all PKA molecules within a cell and not just those involved in guanylin-peptide signalling, and/or (iii) numerous cellular pathways are involved in the response, not just those regulated by PKA. Perhaps, pre-treatment with H-89 prior to RGN addition results in the modulation of multiple intracellular pathways that relate to osmoregulation and cAMP/PKA. Consequently, the effect of H-89 might not be clear and its effects already masked once RGN is added, whereas this might not be the case with post-H-89 after RGN treatment.

PKA inhibition alone (in the absence of RGN) also decreases the absorptive I_{SC} and *TEP*, a result that is not surprising, given the ubiquitous involvement of cAMP and PKA in cellular processes, including ion transport mechanisms. For example, cAMP/PKA has been implicated in NKCC2 stimulation in the Gulf toadfish and sea bream (*Sparus aurata* L,) intestine (Carvalho *et al.*, 2012; Tresguerres *et al.*, 2010) and PKA has been shown to phosphorylate NKCC2 in the thick ascending limb of rats (Ares *et al.*, 2011); both of these mechanisms stimulate ion absorption. Accordingly, their inhibition would reduce ion absorption, similarly to what is observed in the posterior intestine of Gulf toadfish.

Although it is beyond the scope of the present study, RGN activation of GC-C (which has intrinsic GC activity) increases intracellular cGMP formation in fish (Yuge *et al.*, 2006) and mammals (Forte *et al.*, 1993), whose effect in this signalling pathway seems to be mediated more by PKA than PKG. Indeed, in T_{84} cells (which originate from human colon carcinomas), stimulation of GC-C by either STa (the heat-stable *Escherichia coli* enterotoxin that also activates GC-C) or guanylin elevates cGMP formation, leading to changes in cellular physiology, but whose effects are negated by PKA inhibition (Chao *et al.*, 1994). Previous research suggests that there are two possible pathways by which increased cGMP formation is primarily mediated downstream by PKA. The first is indirect activation by inhibition of phosphodiesterase 3 (which cleaves cAMP to its inactive, linear form, AMP) that allows the accumulation of cAMP (Arshad, and Visweswariah, 2013). The second is a putative pathway by which cGMP directly activates PKA, which is suggested to occur in the Japanese tree frog (*Hyla japonica*), after stimulation of urinary bladder cells by atrial natriuretic peptide (Yamada *et al.*, 2006; Yamada *et al.*, 2007). Whatever the pathway might be, prior research on the winter flounder demonstrates that PKA plays a prominent role in intestinal physiology (using VIP and cAMP, both of which are upstream regulators of PKA) by inhibiting ion transport and producing secretory currents (O'Grady S, 1989; O'Grady *et al.*, 1988; Rao *et al.*, 1984). Accordingly, PKA is a possible candidate for mediating the intracellular effects of the guanylin peptides in seawater teleosts.

RGN stimulation leads to increased apical CFTR activation and trafficking

This is the first study to reveal membrane trafficking of CFTR in the Gulf toadfish that is stimulated by RGN. Although it merits further study, RGN can lead to CFTR translocation (present study) or modulate CFTR ion transport (Ruhr *et al.*, 2014). Both of these mechanisms are supported by mammalian and fish studies. In the villi of the rat jejunum, STa and cAMP induce CFTR translocation to the apical membrane and their effects are decreased by PKA inhibition (Golin-Bisello *et al.*, 2005). Likewise, the regulation of CFTR by cAMP/PKA pathways has also been documented in several fish species. For example, in the opercular epithelium of killifish and in the rectal gland of spiny dogfish shark (*Squalus acanthias*), cAMP/PKA has been implicated in CFTR activation (de Jonge *et al.*, 2014; Marshall *et al.*, 2005). Correspondingly, the present study also shows that RGN stimulation increases CFTR translocation to the apical membrane and that the translocation is inhibited by PKA inhibition, similarly to what is displayed by the rat jejunum (Golin-Bisello *et al.*, 2005). Additionally, stimulation of Gulf toadfish posterior intestinal tissues by RGN leads to Cl^- efflux (Ruhr *et al.*, 2015; Ruhr *et al.*, 2016) and is mediated by CFTR (Ruhr *et al.*, 2014). Moreover, due to the short duration of the experiments, in which tissues were treated with RGN between 70-140 min, it is unlikely that the changes in membrane-localized CFTR observed during RGN treatment could be due to changes in protein expression. Indeed, in a previous study on the Gulf toadfish intestine, exposure to 60 ppt seawater eventually increased CFTR mRNA expression, to levels of significance, after 24 h, but not before 12 h (Ruhr *et al.*, 2015). Although the present study does not definitively show CFTR in the apical membrane of the Gulf toadfish intestine, we have previously shown that blocking CFTR with an inhibitor prevents the reversal of the absorptive I_{SC} by RGN when applied to the apical membrane (Ruhr *et al.*, 2014), while its basolateral application has no effect (personal observations). Accordingly, the combined evidence using CFTR inhibition (Ruhr *et al.*, 2014), apical immunofluorescence in the intestine [present and previous studies (Ruhr *et al.*, 2014)], and Western blots on membrane fragments (present study) is compelling in proposing an apical localization of CFTR in the Gulf toadfish intestine. Moreover, there exists the possibility of more than one CFTR isoform being expressed in the Gulf toadfish intestine, as occurs in the Japanese eel (Wong *et*

al., 2016), which could be regulated differently by RGN. Taken together, the current and previous (Ruhr *et al.*, 2014) studies on the Gulf toadfish posterior intestine support the idea that RGN both activates membrane-present CFTR and increases CFTR trafficking to the apical membrane. On a final note, as with many biological mechanisms, CFTR trafficking might be regulated by proteins other than cAMP/PKA. An example relevant to the present study is serum and glucocorticoid-regulated kinase 1 (SGK1), which is a well-known osmotic stress transcription factor found in many vertebrates, including the fish intestine (Wong *et al.*, 2014). SGK1 protein abundance is elevated in the intestine of killifish upon transfer to seawater from freshwater, an increase that is absent by morpholino gene knockdown (Notch *et al.*, 2011). When SGK1 protein synthesis is suppressed in this manner, there is also a corresponding suppression of CFTR insertion into the plasma membrane of the intestine during seawater exposure (Notch *et al.*, 2011). These results are similar to observations in the present study and beg the question: what other possible proteins, enzymes, or intracellular pathways does guanylin peptide stimulation modulate? Undoubtedly, more research on this topic must be carried out.

Does RGN affect SLC26a6 activity and HCO_3^- transport?

In the present and previous studies, posterior intestinal tissues from Gulf toadfish display decreased HCO_3^- secretion when exposed to RGN (Ruhr *et al.*, 2014; Ruhr *et al.*, 2015; Ruhr *et al.*, 2016). However, the mechanism by which this occurs is unknown, although, it is suggested that it involves SLC26a6 (Ruhr *et al.*, 2016), which is the major HCO_3^--secretory transporter in the Gulf toadfish intestine (Grosell, 2006). The present study looked at the possible effect of RGN on the relationship between PKA and HCO_3^- secretion. In the presence of RGN alone, the posterior intestine of Gulf toadfish displays decreased HCO_3^- secretion. However, if tissues are pre-treated with the PKA inhibitor prior to RGN addition, then the effect of RGN on HCO_3^- secretion is almost half than when RGN is added alone (17.5 ± 3.9% decrease with RGN alone vs. 9.6 ± 3.3% with RGN + H-89). These data suggest that decreases in HCO_3^- secretion might be partially mediated by elevated PKA activity, as a result of RGN stimulation. This mechanism is similar to what has been proposed in mammalian models, in which the secondary

messengers – cAMP and PKC – inhibit SLC26 transporters by internalization (Kato, and Romero, 2011). Nevertheless, it is still unknown which HCO_3^- transporter is affected by the downstream effects of RGN, since there are additional bicarbonate transporters (SLC26a3 and SLC4a2) other than SLC26a6 present in the apical membrane (Grosell, 2011). Despite this gap in knowledge, there exist further comparable mechanisms for decreasing HCO_3^- secretion in other animals. Indeed, in the sea bream, stimulation of putative soluble adenylyl cyclase (sAC) that would produce cAMP in intestinal tissues results in increased HCO_3^- secretion (Carvalho *et al.*, 2012), possibly mediated by PKA. For mammals, there is a larger body of work that corroborates what has been seen in fish [see reviews or studies on the pancreas (Ishiguro *et al.*, 2012), exocrine glands (Hong *et al.*, 2014), and intestine (Ko *et al.*, 2002)]. In rat renal proximal tubular epithelial cells, both a cAMP analog and forskolin increase HCO_3^- secretion that is believed to elevate the exchange activity of SLC26a6; these stimulatory effects are inhibited by PKA inhibition via H-89 (Simão *et al.*, 2008). Conversely, to our knowledge, only one study has demonstrated the direct effects of phosphorylation on SLC26a6 exchange activity. It reveals that PKC phosphorylates human SLC26a6, leading to the disruption of a metabolon between the SLC26a6 and carbonic anhydrase II, which decreases HCO_3^- secretion (Alvarez *et al.*, 2005). However, this latter study investigated the role of PKC, as opposed to the present study, which looked at the effects of PKG and PKA on HCO_3^- secretion. Overall, these previous and present studies support the hypothesis that RGN decreases HCO_3^- secretion in Gulf toadfish intestine, possibly by stimulating PKA activity, but the exact intracellular mechanisms by which they occur are still unclear.

Conclusions

The present study reveals that RGN stimulation of the posterior intestine appears to elevate PKA activity (Fig. 7). Upon binding to its receptor, RGN could regulate HCO_3^- and Cl^- transport by modifying potential interactions between SLC26 transporters and CFTR in the Gulf toadfish, as described in the rat intestine. Briefly, the rat intestinal model proposes that SLC26 transporters and CFTR form complexes that interact with one another through binding proteins, and that SLC26 transporters regulate CFTR

activity (Ko *et al.*, 2004). However, there are two main differences between the rat and Gulf toadfish, with respect to HCO_3^- transport and the direction of Cl^- movement through CFTR. In the rat intestine, stimulation of HCO_3^- secretion by SLC26 transporters also stimulates Cl^- absorption by CFTR (Ko *et al.*, 2004), conversely, in the Gulf toadfish intestine, inhibition of HCO_3^- secretion correlates with stimulated Cl^- secretion by CFTR in the Gulf toadfish (Ruhr *et al.*, 2014; Ruhr *et al.*, 2015). Alternatively, the effect of RGN stimulation could be mediated by PKA acting within intracellular microdomains (co-assemblages of proteins) that affects local signalling. Although speculative in the present context (and requiring further study), the presence of microdomains would be advantageous, as they allow endogenous stimulators (e.g. hormones) to activate specific intracellular pathways that are targeted by cAMP and PKA, rather than all pathways involving these molecules (Cooper, 2003; Zaccolo *et al.*, 2006).

Overall, the present study demonstrates that PKA is potentially mediating the downstream effects of RGN in the Gulf toadfish intestine by decreasing HCO_3^- secretion, inhibiting absorptive ion transport, and increasing CFTR trafficking to the apical membrane. Although it is tempting to speculate that this response is associated with GC-Cs in Gulf toadfish intestinal tissues, RGN could also be operating via other receptors evolved to mediate RGN or other guanylin-like peptides. Regardless of which receptor mediates the guanylin-peptide response, previous research on the seawater teleost intestine shows that guanylin-peptide stimulation leads to a reversal of net ion flux (from absorption to secretion) and decreased HCO_3^- secretion, with the overall effect of inhibited (or reversed) water absorption by the intestine (Ando, and Takei, 2015; Ando *et al.*, 2014; Ruhr *et al.*, 2014; Ruhr *et al.*, 2015; Ruhr *et al.*, 2016; Yuge, and Takei, 2007). These effects appear to occur by inhibited NKCC2 transport, activation of CFTR and Cl^- secretion, and inhibited HCO_3^-/Cl^- exchange activity (Ruhr *et al.*, 2014; Ruhr *et al.*, 2016). However, the present study reveals that these changes to ion flux might be a function of CFTR insertion into the apical membrane that is mediated, in part, by PKA, as well as the direct effects on membrane-present CFTR function. Despite what is known about the guanylin peptides in seawater teleosts, their functional importance to whole-animal physiology is still unclear and merit further study.

List of symbols and abbreviations

cAMP: Cyclic adenosine monophosphate

CFTR: Cystic fibrosis transmembrane conductance regulator

cGMP: Cyclic guanosine monophosphate

GC-C: Guanylyl cyclase-C

G_{TE}: Transepithelial conductance

H-89: PKA inhibitor

I_{SC}: Short-circuit current

KT5823: PKG inhibitor

NBCe: Electrogenic sodium-bicarbonate co-transporter

NHE: Sodium-hydrogen exchanger

NKCC2: Sodium-potassium-chloride-chloride symporter

PKA: Protein kinase A

PKG: Protein kinase G

PKI: PKA inhibitor

RGN: Renoguanylin

SLC26a6: Solute Carrier Family 26 Member 6 (HCO_3^-/Cl^--antiporter)

TEP: Transepithelial potential

Acknowledgements

We thank Drs. M. Danielle McDonald and Michael C. Schmale from the Rosenstiel School of Marine and Atmospheric Science at the University of Miami for the generous use of their equipment. M. Grosell is Maytag Professor of Ichthyology and is supported by NSF (IOS 1146695).

Fig. 1. Membrane protein isolations. Western blots (n = 3) for isolated fractions of the posterior intestine from Gulf toadfish reveal specific banding for the Na^+/K^+-ATPase (NKA) (A) and the cystic fibrosis transmembrane conductance regulator (CFTR) (B). NKA is highly enriched in the membrane fraction (M), and much less so in whole cell fraction (W), while it was undetectable in the cytoplasmic fraction (C).

Fig. 2. Modulation of electrophysiology in the posterior intestine. Short-circuit current (I_{SC}) (A) and transepithelial conductance (G_{TE}) (B) displayed by the posterior intestine of Gulf toadfish before and after treatment with renoguanylin (RGN) and combined treatment with RGN and KT5823 (a protein kinase G inhibitor). Pre-treatment values are taken from the final 30 min of the control flux and post-treatment values are taken from the final 30 min of a 70-min treatment flux. Values are means ± SEM (n = 8). Significant differences were revealed by one-way, repeated measures ANOVAs, followed by one-tailed Holm-Sidak tests ($^{a, b}P \leq 0.05$). Positive and negative I_{SC} values indicate secretory and absorptive currents, respectively. RGN (0.1 μmol l^{-1}, dissolved in H_2O) and KT5823 (2 μmol l^{-1}, dissolved in EtOH, final v/v of 0.05%) were added to the mucosal half-chamber of the Ussing apparatus.

Fig. 3. Modulation of electrophysiology in the posterior intestine. Short-circuit current (I_{SC}) (A, B) and transepithelial conductance (G_{TE}) (B, D) displayed by the posterior intestine of Gulf toadfish. The first experiment (A, C) looked at the effects of renoguanylin (RGN) alone, followed by the addition of H-89 (a protein kinase A inhibitor). The second experiment (C, D) looked at the effects of H-89 alone, followed by the addition of RGN. Dimethyl sulfoxide (DMSO) vehicles, in which H-89 stocks were prepared, had no effect on I_{SC} and G_{TE} (E, F). Pre-treatment values are taken from the final 30 min of the control flux and post-treatment values (including DMSO) are taken from the final 30 min of a 70-min treatment flux. Values are means ± SEM (n = 6 for all experiments). Significant differences were revealed by one-way, repeated measures ANOVAs, followed by one-tailed Holm-Sidak tests ($^{a, b, c}P \leq 0.05$). Positive and negative I_{SC} values indicate secretory and absorptive currents, respectively. RGN (0.1 μmol l^{-1}, dissolved

528 in H_2O) and H-89 (20 μmol l^{-1}, dissolved in DMSO, final v/v of 0.1%) were added to the mucosal half-
529 chamber of the Ussing apparatus.
530
531 **Fig. 4. RGN-stimulated CFTR translocation.** A representative Western blot demonstrates differennces
532 in banding intensities [with representative Coomassie staining signals in arbitrary units (a.u.)] in isolated
533 plasma membrane fragments of the posterior intestine of the Gulf toadfish (A). Whole intestinal segments
534 were placed in Ussing chambers and treated with a vehicle (control), renoguanylin (RGN), and RGN + H-
535 89 (a protein kinase A inhibitor) on the mucosal side. Quantification of membrane-present cystic fibrosis
536 transmembrane conductance regulator CFTR banding intensity is shown (B). Renoguanylin (0.1 μmol l^{-1},
537 dissolved in H_2O) treatment increases trafficking of CFTR to the plasma membrane of enterocytes from
538 the posterior intestine, but this movement is inhibited by the presence of H-89 (20 μmol l^{-1}, dissolved in
539 DMSO, final v/v of 0.1%). Values are means ± SEM [n = 3 (9 individuals pooled into three groups)].
540 Significant differences were revealed by a one-way ANOVA, followed by Holm-Sidak tests (*$P \leq 0.05$).
541
542 **Fig. 5. Immuno-location of CFTR.** Immunohistochemsitry reveals that renoguanylin induces increased
543 trafficking of the cystic fibrosis transmembrane conductance regulator (CFTR) to plasma membrane of
544 the enterocytes from the posterior intestine of the Gulf toadfish. Overlaid fluorescence images of 4-μm
545 sections from the posterior intestine of the Gulf toadfish show CFTR (blue) and the Na^+/K^+-ATPase
546 (green). Sections from control (A, C) and renoguanylin-treated tissues (B) reveal different CFTR
547 fluorescence intensity. The brush border is more clearly seen in the lower left panel (C), demonstrating
548 the location of the CFTR immunofluorescence in apical and sub-apical areas. Relative corrected apical
549 fluorescence for the cystic fibrosis transmembrane conductance regulator (CFTR) calculated from
550 fluorescent images of the posterior intestine of Gulf toadfish. Tissues treated with renoguanylin (RGN)
551 display greater CFTR fluorescence relative to control tissues (C). Images are representative of each
552 treatment group (n = 4 each) and shown in 40x (A, B) and 60x (C) magnification. Values are means ±

SEM and significant differences were revealed by a Student's t-test (*$P \leq 0.05$). Abbreviations: A (apical membrane), B (basolateral membrane), L (lumen), BB (brush border).

Fig. 6. Modulation of HCO_3^- secretion. HCO_3^- secretion (A, C), and transepithelial potential (TEP) and transepithelial conductance (G_{TE}) (B, D) displayed by the posterior intestine of Gulf toadfish. Control values were taken from the final 30 min of the control flux. Renoguanylin (RGN) or H-89 (a protein kinase A inhibitor) was then added, and its effects were measured from the final 30 min of a 70-min treatment flux. Finally, H-89 or RGN was added in combination to the first treatment, and their overall effects were measured from the final 30 min of a 70-min treatment flux (t_{total} = 170 min). Values are means ± SEM. Significant differences were revealed by one-way, repeated measures ANOVAs, followed by Holm-Sidak tests ($^{a, b, c}P \leq 0.05$). Positive and negative TEP values indicate net anion secretion and absorption, respectively. RGN (0.1 μmol l^{-1}, dissolved in H_2O) and H-89 (20 μmol l^{-1}, dissolved in DMSO, final v/v of 0.1%) were added to the mucosal half-chamber of the Ussing apparatus.

Fig. 7. Intracellular effects of guanylin peptides. Simplified proposed effects of the guanylin peptides in the enterocytes of the posterior intestine of Gulf toadfish (*Opsanus beta*). Guanylin (GN), uroguanylin (UGN), and renoguanylin (RGN) bind to a guanylyl cyclase-C (GC-C) receptor on the apical membrane of an enterocyte. The stimulation of GC-C, which has intrinsic GC activity, leads to enhanced formation of cyclic guanosine monophosphate (cGMP), whose downstream effects appear to stimulate protein kinase A (PKA) activity. Stimulation of GC-C causes an increase in PKA activity that (i) reduces HCO_3^- secretion, possibly by altering the HCO_3^-/Cl^- exchange activity (in the case of the Gulf toadfish, this would occur primarily by inhibiting SLC26a6 transport), (ii) this also triggers the opening of membrane-present cystic fibrosis transmembrane conductance regulator (CFTR) Cl^- channels (either through direct phosphorylation by PKA or due to interactions with SLC26a6), and (iii) insertion of CFTR into the plasma membrane. From previous studies on teleost fish, the combined effects of GC-C stimulation

579 results in the reversal of ion flux, from net ion absorption (mucosa-to-serosa) to net ion secretion (serosa-
580 to-mucosa) that leads to inhibited water absorption (Ruhr *et al.*, 2014; Ruhr *et al.*, 2015; Ruhr *et al.*,
581 2016). Abbreviations/symbols: TJ (tight junction), stimulatory (+) and inhibitory (-) effects.

582 **Table 1. Composition of salines for short-circuit current, pH-stat titration, and sac preparation**

583 **experiments**

Compound	Mucosal*	Serosal†	HCO_3^-/CO_2-free serosal
NaCl, mmol l^{-1}	169.0	151.0	151.0
KCl, mmol l^{-1}	5.0	3.0	3.0
$MgSO_4$, mmol l^{-1}	77.5	0.88	0.88
$MgCl_2$, mmol l^{-1}	22.5		
Na_2HPO_4, mmol l^{-1}		0.5	0.5
KH_2PO_4, mmol l^{-1}		0.5	0.5
$CaCl_2$, mmol l^{-1}	5.0	1.0	1.0
$NaHCO_3$, mmol l^{-1}		5.0	
HEPES, free acid, mmol l^{-1}		11.0	11.0
HEPES, Na^+ salt, mmol l^{-1}		11.0	11.0
Urea, mmol l^{-1}		4.5	4.5
Glucose, mmol l^{-1}		5.0	5.0
Osmolality§, mosmol/kg H_2O	330	330	330
pH	7.8†	7.8	7.8
Gas‡	100% O_2	0.3% CO_2 in O_2	100% O_2

*Mucosal application of blockers and pharmaceuticals: Renoguanylin was added to a final concentration of 10^{-7} and 5 x 10^{-7} mol l^{-1} in Ussing chamber and sac preparation experiments, respectively. Bumetanide and ethoxzolamide were added to Ussing chambers for final concentrations of 10 and 100 μmol l^{-1}, respectively. Salines were adjusted for osmolality with mannitol (§). When measuring HCO_3^- secretion, mucosal pH in Ussing chambers was maintained at 7.8 by pH-stat titration (†). Salines were gassed for at least 1 h prior to experiments (‡).

584

585

Table 2. p-values for the results of two-tailed Holm-Sidak tests used in the present study

Corresponding Figure	Variable	Comparison	Two-tailed p-value
2A	I_{sc}	RGN vs. control	<0.001
		KT5823 vs. control	<0.001
2B	G_{TE}	RGN vs. control	<0.001
		KT5823 vs. control	<0.001
3A	I_{sc}	RGN vs. control	<0.001
		RGN + H-89 vs. control	<0.001
		RGN vs. RGN + H-89	0.01
3B	G_{TE}	RGN vs. control	0.003
		RGN + H-89 vs. control	0.05
		RGN vs. RGN + H-89	0.065
3C	I_{sc}	H-89 vs. control	<0.001
		H-89 + RGN vs. control	<0.001
		H-89 vs. H-89 RGN	0.001
3D	G_{TE}	H-89 vs. control	<0.001
		H-89 + RGN vs. control	0.023
		H-89 vs. H-89 + RGN	<0.001
4B	Band intensity	RGn vs. Control	0.024
6A	HCO_3^- secretion	RGN vs. control	0.034
		RGN + H-89 vs. control	0.002
		RGN vs. RGN + H-89	0.032
6B	TEP	RGN vs. control	0.008
		RGN + H-89 vs. control	0.019
		RGN vs. RGN + H-89	0.031
6B	G_{TE}	RGN vs. control	0.171
		RGN + H-89 vs. control	0.011
		RGN vs. RGN + H-89	0.002
6C	HCO_3^- secretion	H-89 vs. control	0.300
		H-89 + RGN vs. control	0.159
		H-89 vs. H-89 RGN	0.043
6D	TEP	H-89 vs. control	0.002
		H-89 + RGN vs. control	<0.001
		H-89 vs. H-89 RGN	0.232
6D	G_{TE}	H-89 vs. control	0.255
		H-89 + RGN vs. control	0.018
		H-89 vs. H-89 RGN	0.004

References

Alvarez, B. V., Vilas, G. L., and Casey, J. R. (2005). Metabolon disruption: a mechanism that regulates bicarbonate transport. *EMBO J* **24**, 2499-511.

Ando, M., and Takei, Y. (2015). Guanylin activates Cl^- secretion into the lumen of seawater eel intestine via apical Cl^- channel under simulated in vivo conditions. *Am J Physiol Regul Integr Comp Physiol* **308**, R400-R410.

Ando, M., Wong, M. K., and Takei, Y. (2014). Mechanisms of guanylin action on water and ion absorption at different regions of seawater eel intestine. *Am J Physiol Regul Integr Comp Physiol* **307**, R653-63.

Ares, G. R., Caceres, P. S., and Ortiz, P. A. (2011). Molecular regulation of NKCC2 in the thick ascending limb. *Am J Physiol Renal Physiol* **301**, F1143-59.

Arshad, N., and Visweswariah, S. S. (2012). The multiple and enigmatic roles of guanylyl cyclase C in intestinal homeostasis. *FEBS Lett* **586**, 2835-40.

Arshad, N., and Visweswariah, S. S. (2013). Cyclic nucleotide signaling in intestinal epithelia: getting to the gut of the matter. *Wiley Interdiscip Rev Syst Biol Med* **5**, 409-24.

Carvalho, E. S., Gregorio, S. F., Power, D. M., Canario, A. V., and Fuentes, J. (2012). Water absorption and bicarbonate secretion in the intestine of the sea bream are regulated by transmembrane and soluble adenylyl cyclase stimulation. *J Comp Physiol B* **182**, 1069-80.

Chao, A. C., de Sauvage, F. J., Dong, Y. J., Wagner, J. A., Goeddel, D. V., and Gardner, P. (1994). Activation of intestinal CFTR Cl^- channel by heat-stable enterotoxin and guanylin via cAMP-dependent protein kinase. *EMBO J* **13**, 1065-72.

Cooper, D. M. (2003). Regulation and organization of adenylyl cyclases and cAMP. *Biochem J* **375**, 517-29.

Currie, M. G., Fok, K. F., Kato, J., Moore, R. J., Hamra, F. K., Duffin, K. L., and Smith, C. E. (1992). Guanylin: an endogenous activator of intestinal guanylate cyclase. *Proc Natl Acad Sci* **89**, 947-51.

de Jonge, H. R., Tilly, B. C., Hogema, B. M., Pfau, D. J., Kelley, C. A., Kelley, M. H., Melita, A. M., Morris, M. T., Viola, R. M., and Forrest, J. N. (2014). cGMP inhibition of type 3 phosphodiesterase is the major mechanism by which C-type natriuretic peptide activates CFTR in the shark rectal gland. *Am J Physiol Cell Physiol* **306**, C343-C353.

Evans, D. H., Piermarini, P. M., and Choe, K. P. (2005). The multifunctional fish gill: dominant site of gas exchange, osmoregulation, acid-base regulation, and excretion of nitrogenous waste. *Physiol Rev* **85**, 97-177.

Forte, L. R. (1999). Guanylin regulatory peptides: structures, biological activities mediated by cyclic GMP and pathobiology. *Regul Pept* **81**, 25-39.

Forte, L. R., Eber, S. L., Turner, J. T., Freeman, R. H., Fok, K. F., and Currie, M. G. (1993). Guanylin stimulation of Cl^- secretion in human intestinal T84 cells via cyclic guanosine monophosphate. *J Clin Invest* **91**, 2423-8.

Forte, L. R., and Hamra, F. K. (1996). Guanylin and uroguanylin: Intestinal peptide hormones that regulate epithelial transport. *News Physiol Sci* **11**, 17-24.

Golin-Bisello, F., Bradbury, N., and Ameen, N. (2005). STa and cGMP stimulate CFTR translocation to the surface of villus enterocytes in rat jejunum and is regulated by protein kinase G. *Am J Physiol Cell Physiol* **289**, C708-16.

Greenberg, R. N., Hill, M., Crytzer, J., Krause, W. J., Eber, S. L., Hamra, F. K., and Forte, L. R. (1997). Comparison of effects of uroguanylin, guanylin, and *Escherichia coli* heat-

stable enterotoxin STa in mouse intestine and kidney: Evidence that uroguanylin is an intestinal natriuretic hormone. *J Inv Med* **45**, 276-283.

Grosell, M. (2006). Intestinal anion exchange in marine fish osmoregulation. *J Exp Biol* **209**, 2813-27.

Grosell, M. (2011). Intestinal anion exchange in marine teleosts is involved in osmoregulation and contributes to the oceanic inorganic carbon cycle. *Acta Physiol (Oxf)* **202**, 421-34.

Grosell, M., and Genz, J. (2006). Ouabain-sensitive bicarbonate secretion and acid absorption by the marine teleost fish intestine play a role in osmoregulation. *Am J Physiol Regul Integr Comp Physiol* **291**, R1145-56.

Grosell, M., Genz, J., Taylor, J. R., Perry, S. F., and Gilmour, K. M. (2009a). The involvement of H^+-ATPase and carbonic anhydrase in intestinal HCO_3^- secretion in seawater-acclimated rainbow trout. *J Exp Biol* **212**, 1940-8.

Grosell, M., Mager, E., Williams, C., and Taylor, J. (2009b). High rates of HCO_3^- secretion and Cl^- absorption against adverse gradients in the marine teleost intestine: the involvement of an electrogenic anion exchanger and H^+-pump metabolon? *J Exp Biol* **212**, 1684-1696.

Hamra, F. K., Forte, L. R., Eber, S. L., Pidhorodeckyj, N. V., Krause, W. J., Freeman, R. H., Chin, D. T., Tompkins, J. A., Fok, K. F., and Smith, C. E. (1993). Uroguanylin: structure and activity of a second endogenous peptide that stimulates intestinal guanylate cyclase. *Proc Natl Acad Sci* **90**, 10464-10468.

Hong, J. H., Park, S., Shcheynikov, N., and Muallem, S. (2014). Mechanism and synergism in epithelial fluid and electrolyte secretion. *Pflügers Arch* **466**, 1487-99.

Iio, K., Nakauchi, M., Yamagami, S., Tsutsumi, M., Hori, H., Naruse, K., Mitani, H., Shima, A., and Suzuki, N. (2005). A novel membrane guanylyl cyclase expressed in medaka (*Oryzias latipes*) intestine. *Comp Biochem Physiol B Biochem Mol Biol* **140**, 569-578.

Ishiguro, H., Yamamoto, A., Nakakuki, M., Yi, L., Ishiguro, M., Yamaguchi, M., Kondo, S., and Mochimaru, Y. (2012). Physiology and pathophysiology of bicarbonate secretion by pancreatic duct epithelium. *Nagoya J Med Sci* **74**, 1-18.

Kato, A., and Romero, M. F. (2011). Regulation of electroneutral NaCl absorption by the small intestine. *Annu Rev Physiol* **73**, 261.

Ko, S. B., Shcheynikov, N., Choi, J. Y., Luo, X., Ishibashi, K., Thomas, P. J., Kim, J. Y., Kim, K. H., Lee, M. G., and Naruse, S. (2002). A molecular mechanism for aberrant CFTR□dependent HCO_3^- transport in cystic fibrosis. *EMBO J* **21**, 5662-5672.

Ko, S. B., Zeng, W., Dorwart, M. R., Luo, X., Kim, K. H., Millen, L., Goto, H., Naruse, S., Soyombo, A., Thomas, P. J. et al. (2004). Gating of CFTR by the STAS domain of SLC26 transporters. *Nat Cell Biol* **6**, 343-50.

Kuhn, M., Adermann, K., Jahne, J., Forssmann, W. G., and Rechkemmer, G. (1994). Segmental differences in the effects of guanylin and *Escherichia coli* heat-stable enterotoxin on Cl^- secretion in human gut. *J Physiol* **479**, 433-440.

Loretz, C. A. (1995). 2 Electrophysiology of Ion Transport in Teleost Intestinal Cells. *Fish physiology* **14**, 25-56.

Marshall, W. S., Howard, J. A., Cozzi, R. R., and Lynch, E. M. (2002). NaCl and fluid secretion by the intestine of the teleost *Fundulus heteroclitus*: involvement of CFTR. *J Exp Biol* **205**, 745-58.

Marshall, W. S., Ossum, C. G., and Hoffmann, E. K. (2005). Hypotonic shock mediation by p38 MAPK, JNK, PKC, FAK, OSR1 and SPAK in osmosensing chloride secreting cells of killifish opercular epithelium. *J Exp Biol* **208**, 1063-77.

McCormick, S. D., Regish, A. M., and Christensen, A. K. (2009). Distinct freshwater and seawater isoforms of Na^+/K^+-ATPase in gill chloride cells of Atlantic salmon. *J Exp Biol* **212**, 3994-4001.

Notch, E. G., Shaw, J. R., Coutermarsh, B. A., Dzioba, M., and Stanton, B. A. (2011). Morpholino gene knockdown in adult *Fundulus heteroclitus*: role of SGK1 in seawater acclimation. *PLoS One* **6**, e29462.

O'Grady S, M. (1989). Cyclic nucleotide-mediated effects of ANF and VIP on flounder intestinal ion transport. *Am J Physiol Regul Integr Comp Physiol* **256**, C142-6.

O'Grady, S. M., DeJonge, H. R., Vaandrager, A. B., and Field, M. (1988). Cyclic nucleotide-dependent protein kinase inhibition by H-8: effects on ion transport. *Am J Physiol Regul Integr Comp Physiol* **254**, C115-21.

O'Grady, S. M., Field, M., Nash, N. T., and Rao, M. C. (1985). Atrial natriuretic factor inhibits Na-K-Cl cotransport in teleost intestine. *Am J Physiol Regul Integr Comp Physiol* **249**, C531-4.

O'Grady, S. M., and Wolters, P. J. (1990). Evidence for chloride secretion in the intestine of the winter flounder. *Am J Physiol Regul Integr Comp Physiol* **258**, C243-7.

Potapova, T. A., Sivakumar, S., Flynn, J. N., Li, R., and Gorbsky, G. J. (2011). Mitotic progression becomes irreversible in prometaphase and collapses when Wee1 and Cdc25 are inhibited. *Mol Biol Cell* **22**, 1191-1206.

Rao, M. C., and Nash, N. T. (1988). 8-BrcAMP does not affect Na-K-2Cl cotransport in winter flounder intestine. *Am J Physiol Cell Physiol* **255**, C246-C251.

Rao, M. C., Nash, N. T., and Field, M. (1984). Differing effects of cGMP and cAMP on ion transport across flounder intestine. *Am J Physiol Regul Integr Comp Physiol* **246**, C167-71.

Ruhr, I. M., Bodinier, C., Mager, E. M., Esbaugh, A. J., Williams, C., Takei, Y., and Grosell, M. (2014). Guanylin peptides regulate electrolyte and fluid transport in the Gulf toadfish (*Opsanus bet*a) posterior intestine. *Am J Physiol Regul Integr Comp Physiol* **307**, R1167-79.

Ruhr, I. M., Mager, E. M., Takei, Y., and Grosell, M. (2015). The differential role of renoguanylin in osmoregulation and apical Cl^-/HCO_3^- exchange activity in the posterior intestine of the Gulf toadfish (*Opsanus beta*). *Am J Physiol Regul Integr Comp Physiol* **309**, R399-R409.

Ruhr, I. M., Takei, Y., and Grosell, M. (2016). The role of the rectum in osmoregulation and the potential effect of renoguanylin on SLC26a6 transport activity in the Gulf toadfish (*Opsanus beta*). *Am J Physiol Regul Integr Comp Physiol* **311**, R179-91.

Schindelin, J., Arganda-Carreras, I., Frise, E., Kaynig, V., Longair, M., Pietzsch, T., Preibisch, S., Rueden, C., Saalfeld, S., Schmid, B. et al. (2012). Fiji: an open-source platform for biological-image analysis. *Nat Methods* **9**, 676-82.

Schulz, S., Green, C. K., Yuen, P. S., and Garbers, D. L. (1990). Guanylyl cyclase is a heat-stable enterotoxin receptor. *Cell* **63**, 941-948.

Schulze, K. S. (2015). The imaging and modelling of the physical processes involved in digestion and absorption. *Acta Physiol (Oxf)* **213**, 394-405.

Simão, S., Pedrosa, R., Hopfer, U., Mount, D. B., Jose, P. A., and Soares-da-Silva, P. (2008). Short-term regulation of the Cl^-/HCO_3^- exchanger in immortalized SHR proximal tubular epithelial cells. *Biochem Pharmacol* **75**, 2224-2233.

Skadhauge, E. (1969). The mechanism of salt and water absorption in the intestine of the eel (*Anguilla anguilla*) adapted to waters of various salinities. *J Physiol* **204**, 135-158.

Skadhauge, E. (1974). Coupling of transmural flows of NaCl and water in the intestine of the eel (*Anguilla anguilla*). *J Exp Biol* **60**, 535-546.

Tresguerres, M., Levin, L. R., Buck, J., and Grosell, M. (2010). Modulation of NaCl absorption by [HCO_3^-] in the marine teleost intestine is mediated by soluble adenylyl cyclase. *Am J Physiol Regul Integr Comp Physiol* **299**, R62-R71.

Tresguerres, M., Parks, S. K., Wood, C. M., and Goss, G. G. (2007). V-H^+-ATPase translocation during blood alkalosis in dogfish gills: interaction with carbonic anhydrase and involvement in the postfeeding alkaline tide. *Am J Physiol Regul Integr Comp Physiol* **292**, R2012-R2019.

Weber, W. M., Cuppens, H., Cassiman, J. J., Clauss, W., and Van Driessche, W. (1999). Capacitance measurements reveal different pathways for the activation of CFTR. *Pflugers Arch* **438**, 561-9.

Wilson, R. W., Wilson, J. M., and Grosell, M. (2002). Intestinal bicarbonate secretion by marine teleost fish – why and how? *Biochim Biophys Acta Biomemb* **1566**, 182-193.

Wong, M. K.-S., Ozaki, H., Suzuki, Y., Iwasaki, W., and Takei, Y. (2014). Discovery of osmotic sensitive transcription factors in fish intestine via a transcriptomic approach. *BMC genomics* **15**, 1134.

Wong, M. K., Pipil, S., Kato, A., and Takei, Y. (2016). Duplicated CFTR isoforms in eels diverged in regulatory structures and osmoregulatory functions. *Comp Biochem Physiol A Mol Integr Physiol* **199**, 130-41.

Yamada, T., Matsuda, K., and Uchiyama, M. (2006). Atrial natriuretic peptide and cGMP activate sodium transport through PKA-dependent pathway in the urinary bladder of the Japanese tree frog. *J Comp Physiol B* **176**, 203-212.

Yamada, T., Matsuda, K., and Uchiyama, M. (2007). Frog ANP increases the amiloride-sensitive Na^+ channel activity in urinary bladder cells of Japanese tree frog, Hyla japonica. *Gen Comp Endocrinol* **152**, 286-8.

Yuge, S., and Takei, Y. (2007). Regulation of ion transport in eel intestine by the homologous guanylin family of peptides. *Zoolog Sci* **24**, 1222-30.

Yuge, S., Yamagami, S., Inoue, K., Suzuki, N., and Takei, Y. (2006). Identification of two functional guanylin receptors in eel: multiple hormone-receptor system for osmoregulation in fish intestine and kidney. *Gen Comp Endocrinol* **149**, 10-20.

Zaccolo, M., Di Benedetto, G., Lissandron, V., Mancuso, L., Terrin, A., and Zamparo, I. (2006). Restricted diffusion of a freely diffusible second messenger: mechanisms underlying compartmentalized cAMP signalling. *Biochem Soc Trans* **34**, 495-7.

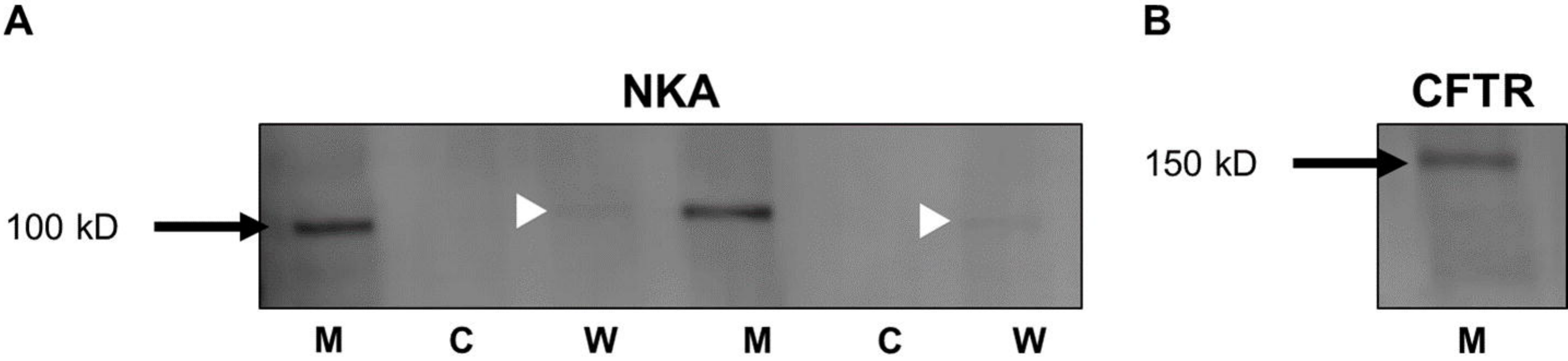
A
NKA
100 kD
M
C
W
M
C
W
B
CFTR
150 kD
M

A

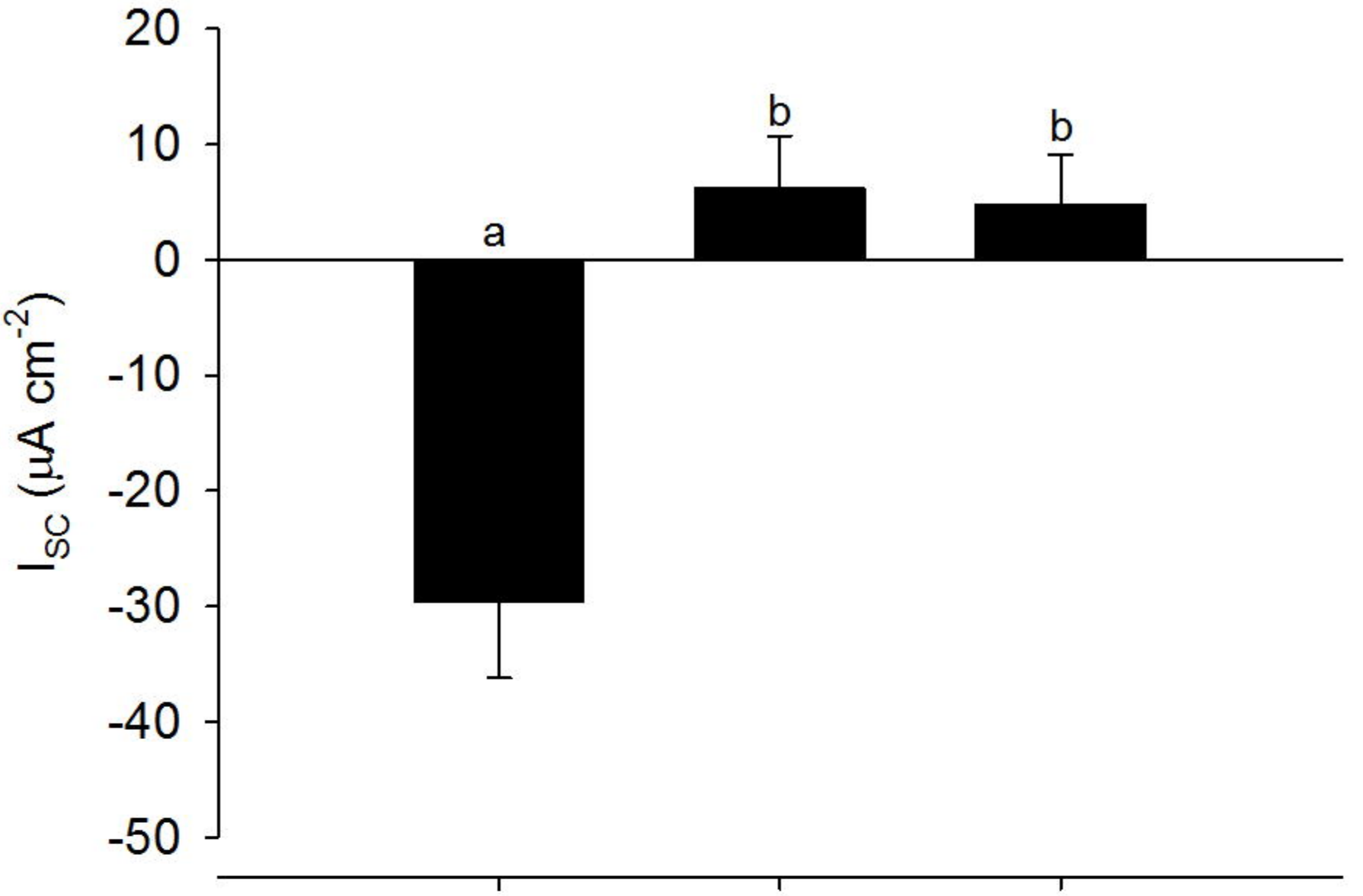
20
10
0
-10
-20
-30
-40
-50
I_{SC} (μA cm^{-2})
a
b
b

B

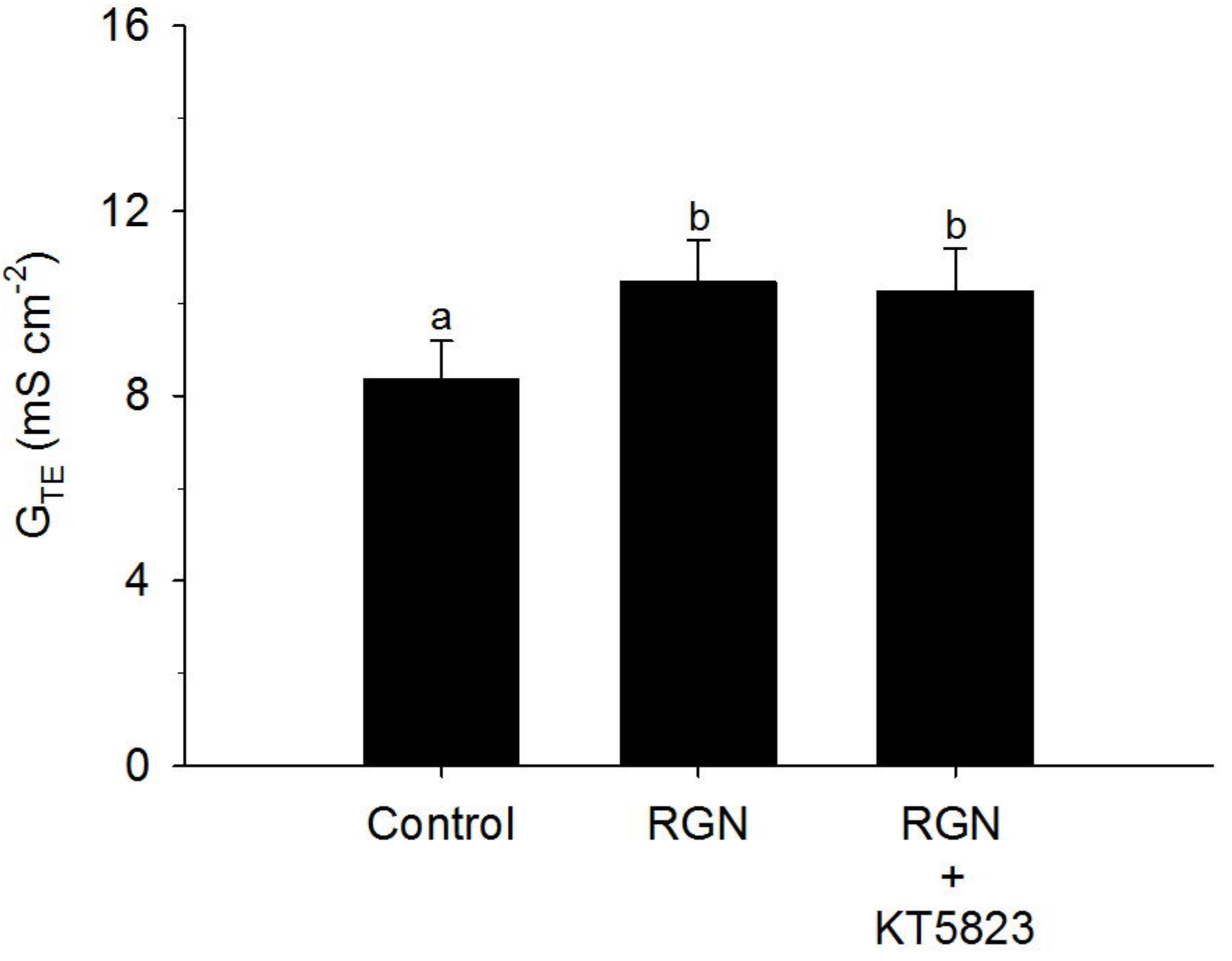
16
12
8
4
0
G_{TE} (mS cm^{-2})
a
b
b
Control
RGN
RGN
+
KT5823

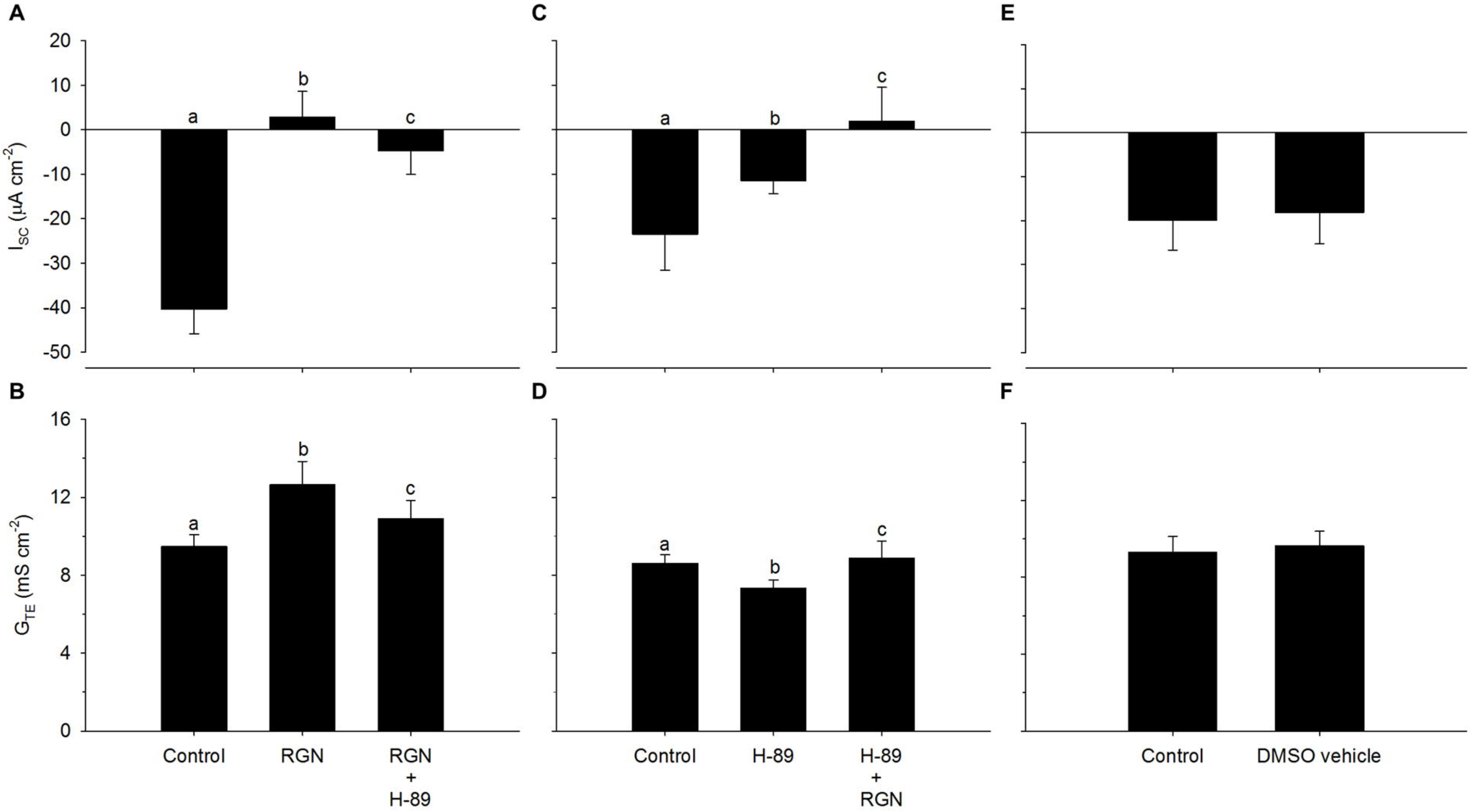
A
C
E
B
D
F
20
10
0
-10
-20
-30
-40
-50
I_{SC} (μA cm^{-2})
16
12
8
4
0
G_{TE} (mS cm^{-2})
a
b
c
Control
RGN
RGN + H-89
H-89
H-89 + RGN
DMSO vehicle

A

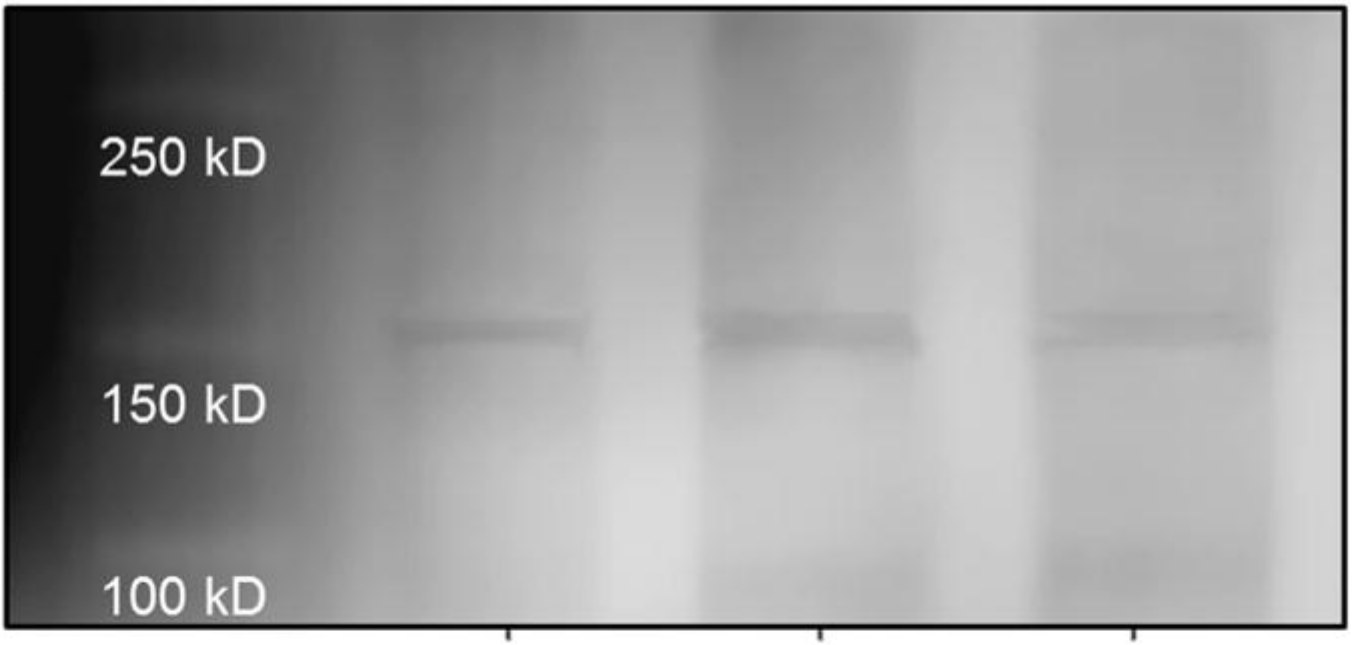

	Corresponding Coomassie staining intensities (a.u.)		
CFTR signal	3,380	4,130	2,900
Whole-protein signal	1,980,000	1,830,000	2,190,000

B

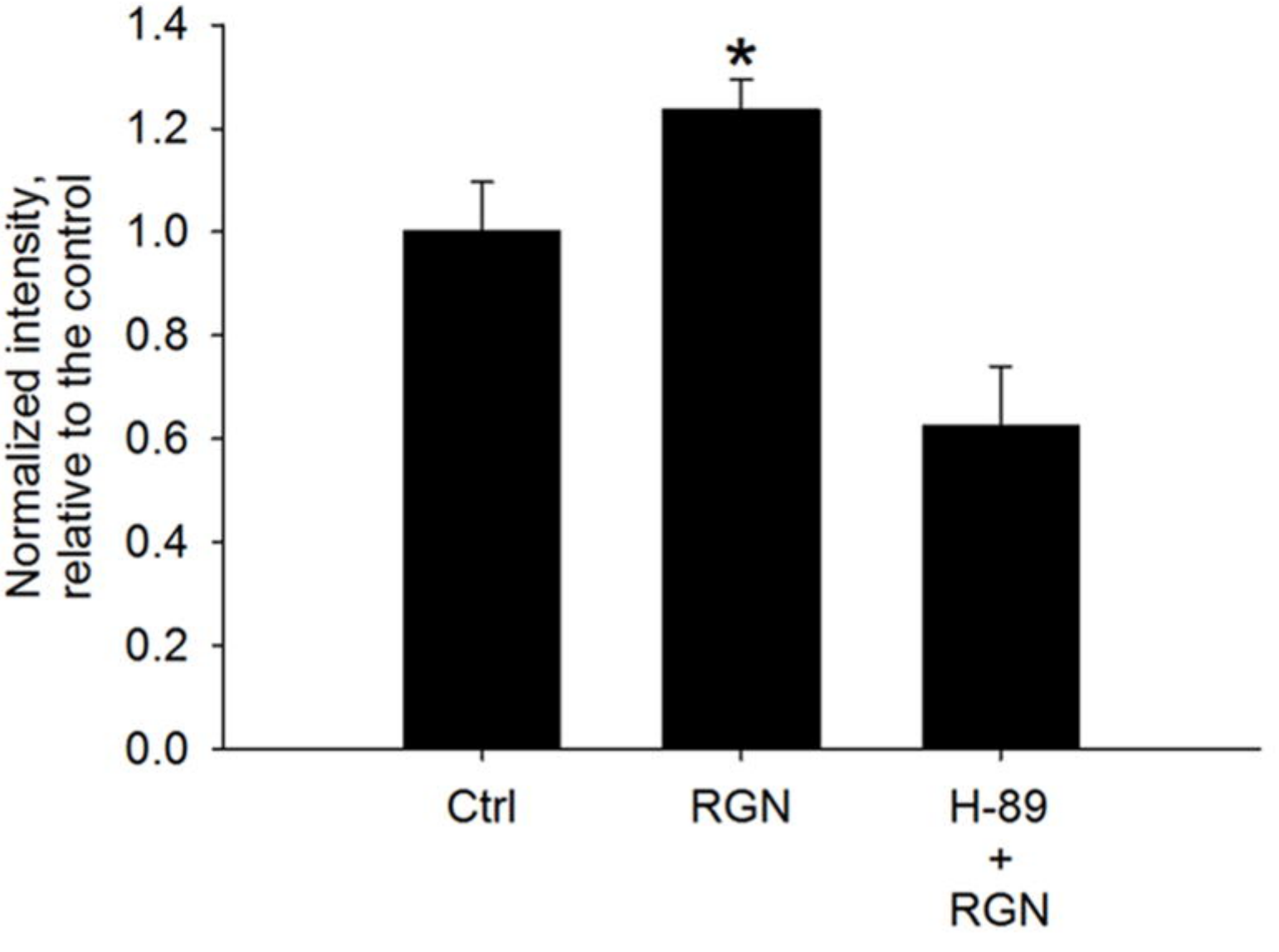

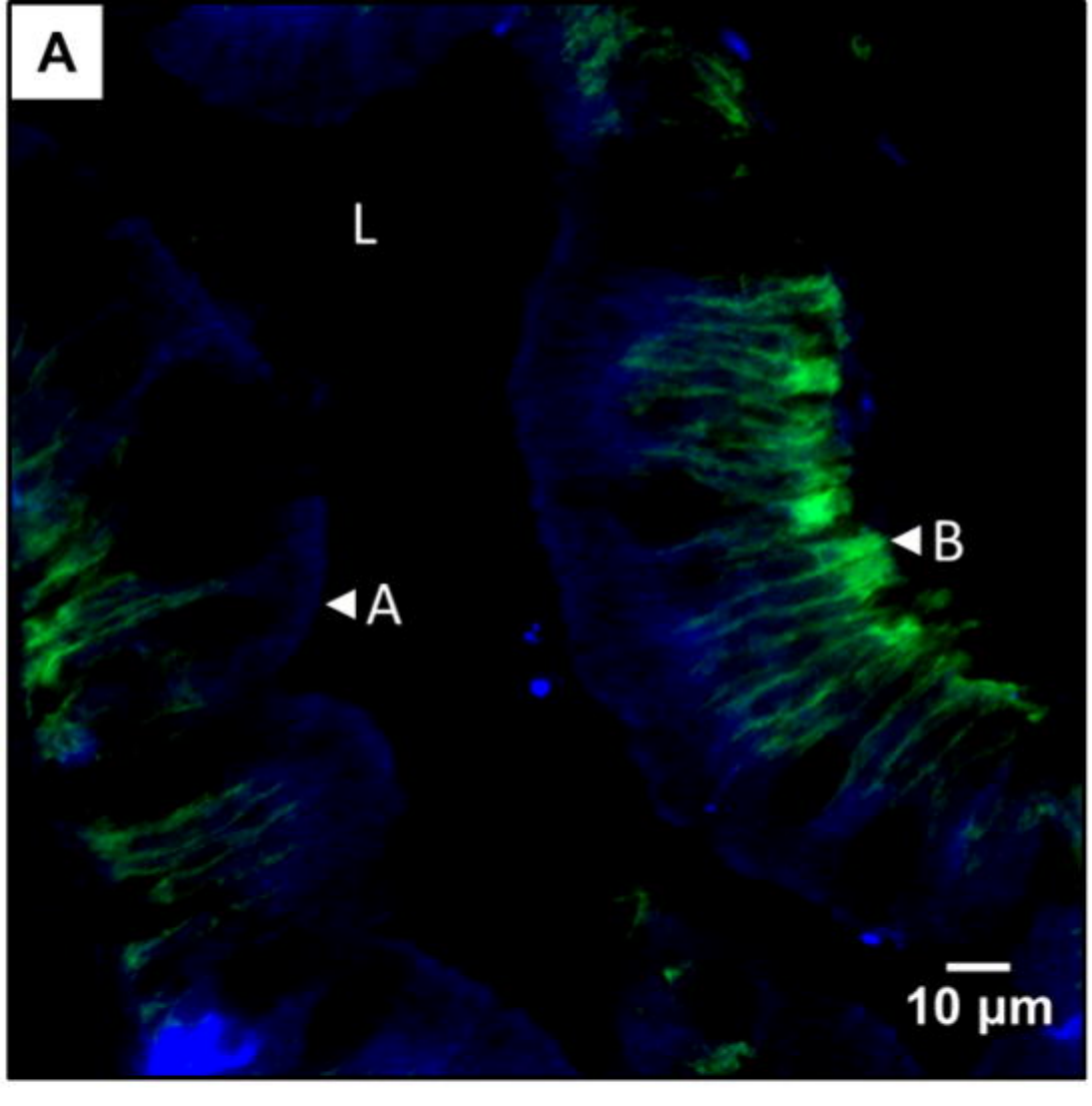
A
L
B
A
10 µm

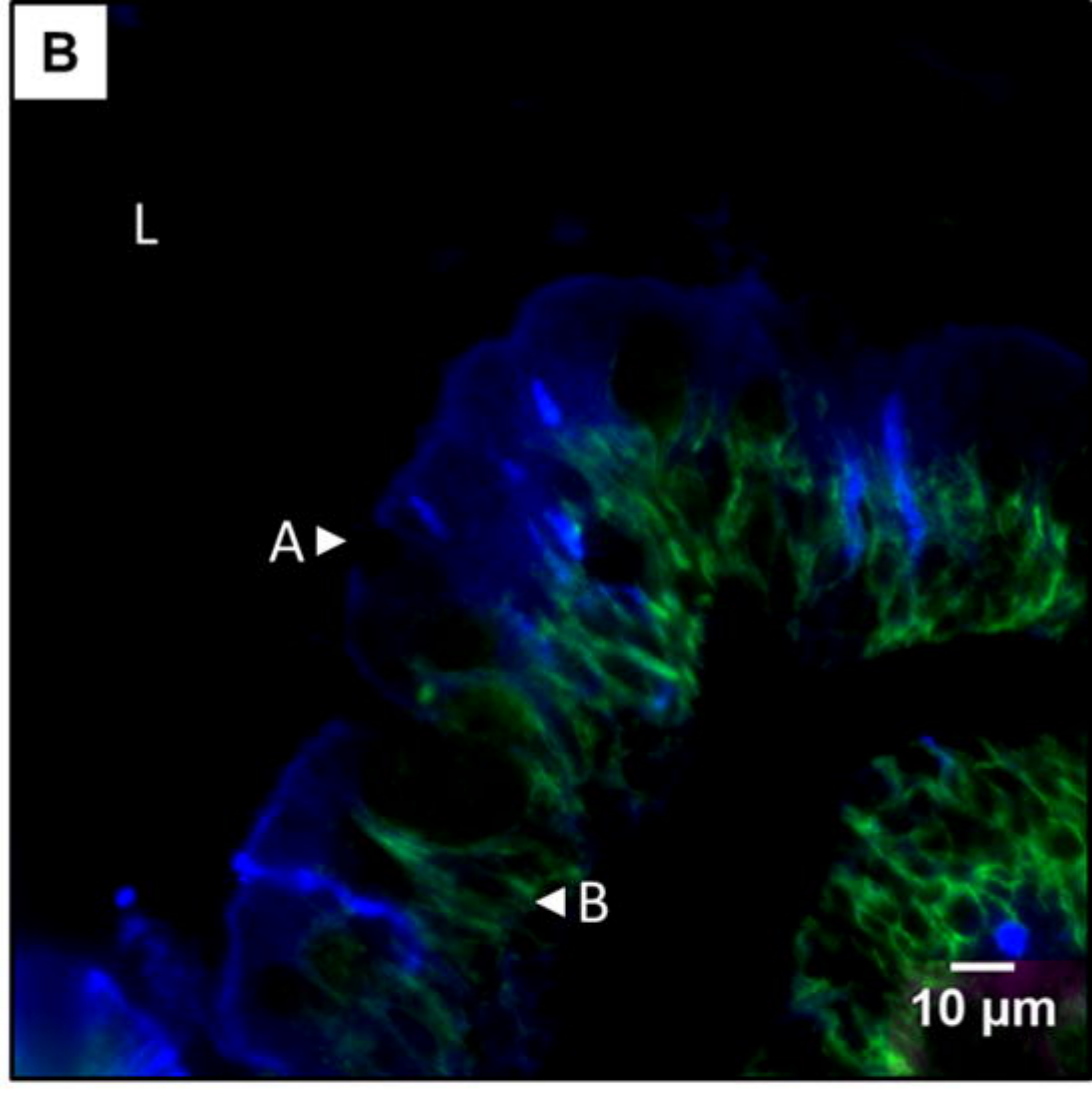
B
L
A
B
10 µm

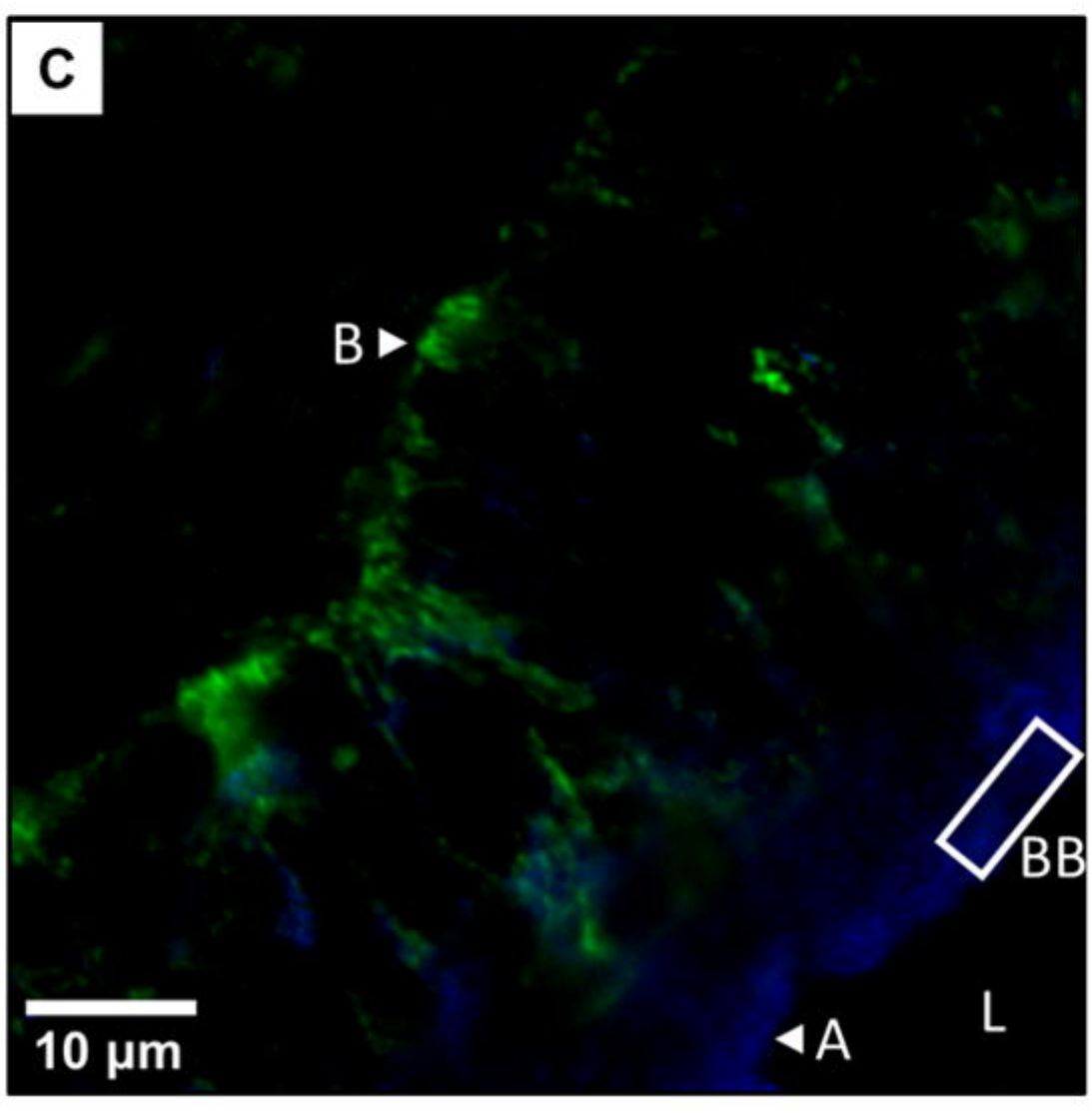
C
B
BB
10 µm
A
L

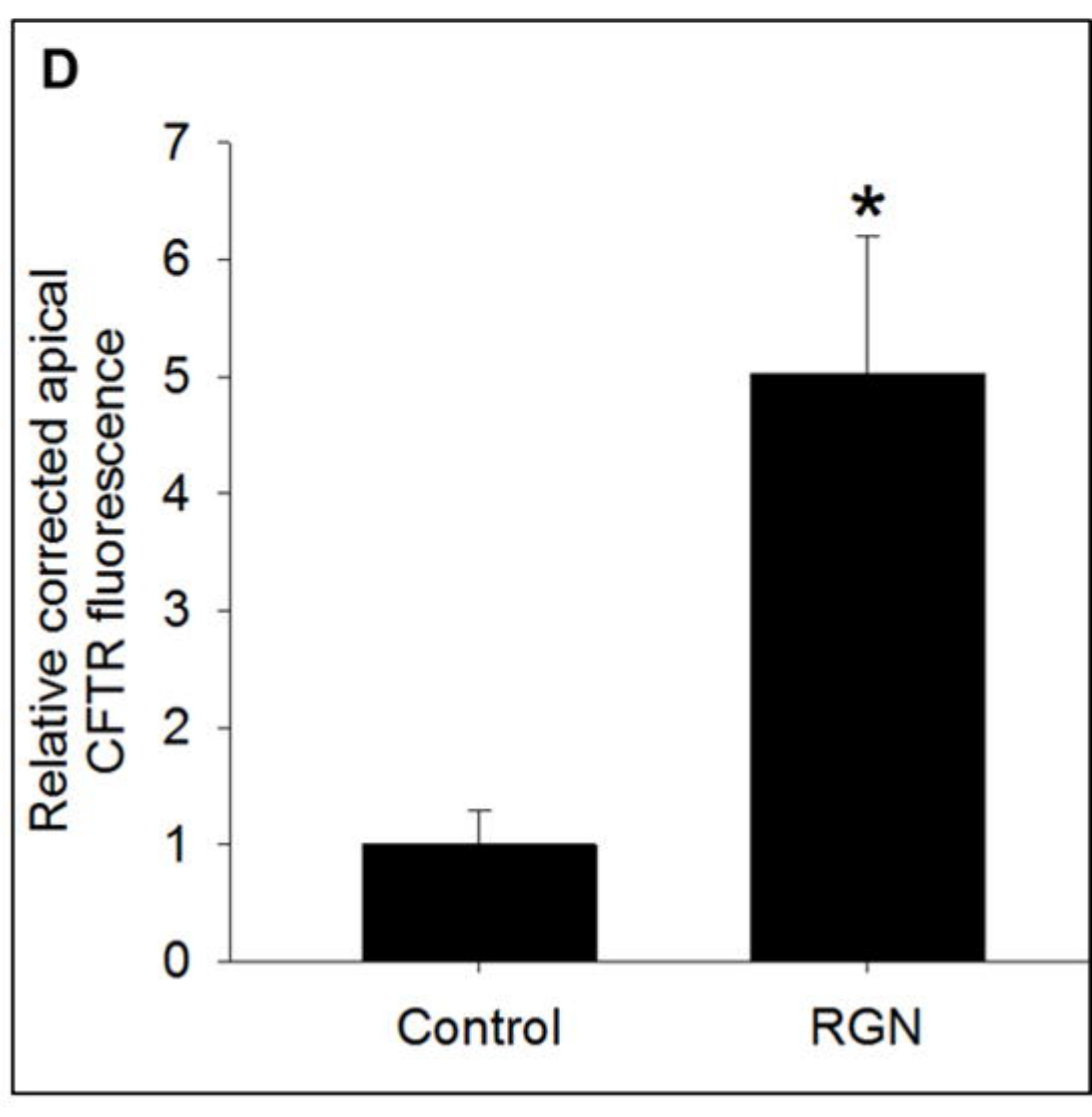
D
Relative corrected apical CFTR fluorescence
0
1
2
3
4
5
6
7
*
Control
RGN

A

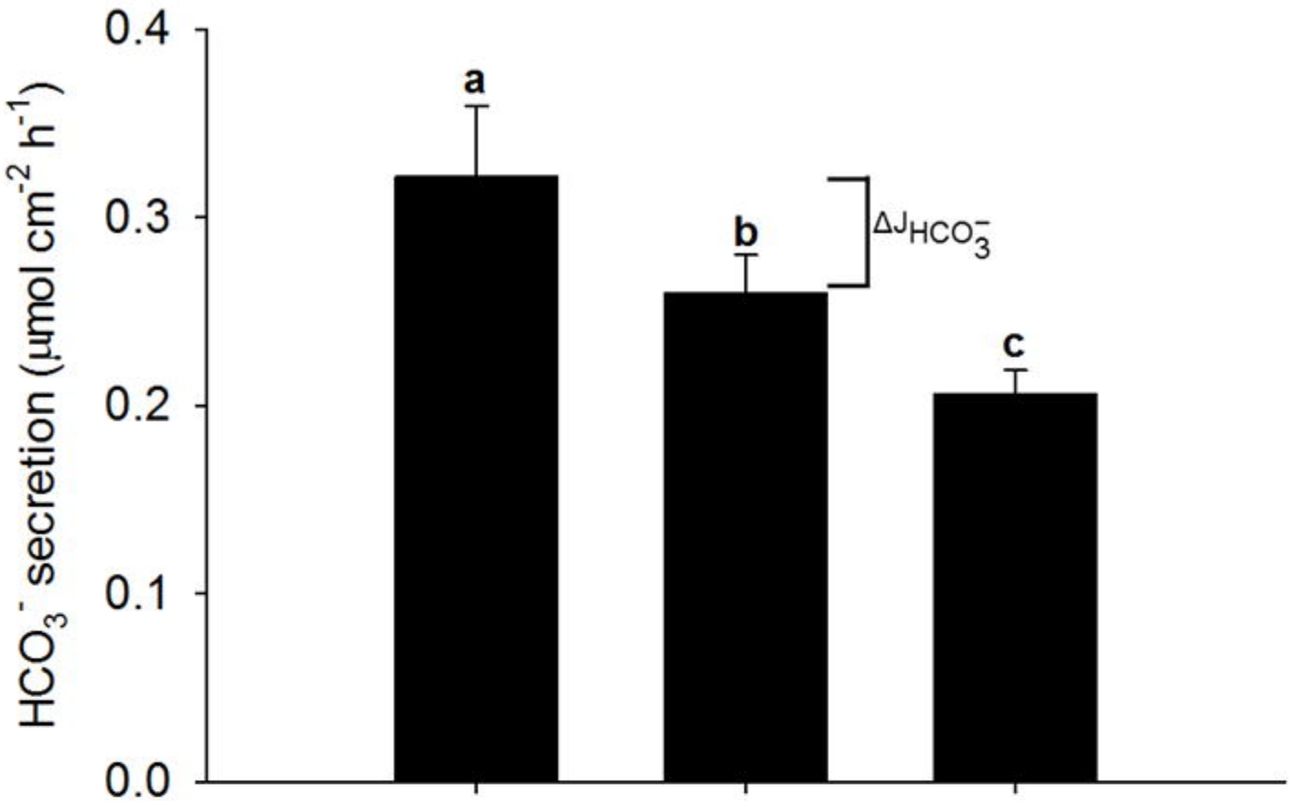
0.4
0.3
0.2
0.1
0.0
HCO_3^- secretion (µmol cm^{-2} h^{-1})
a
b
c
$\Delta J_{HCO_3^-}$

C

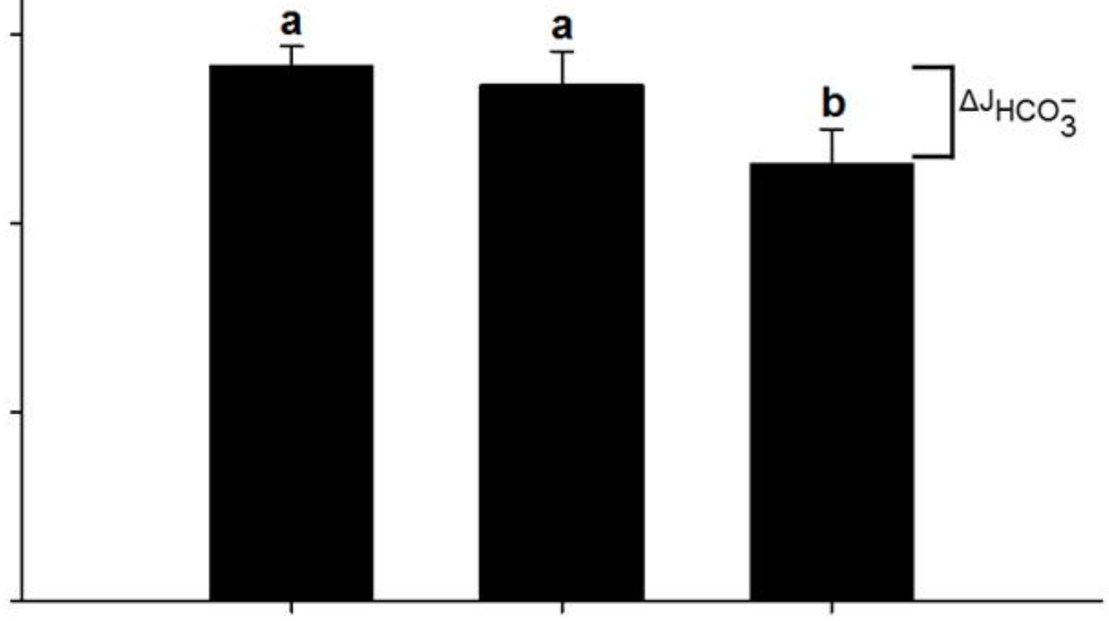
a
a
b
$\Delta J_{HCO_3^-}$

B

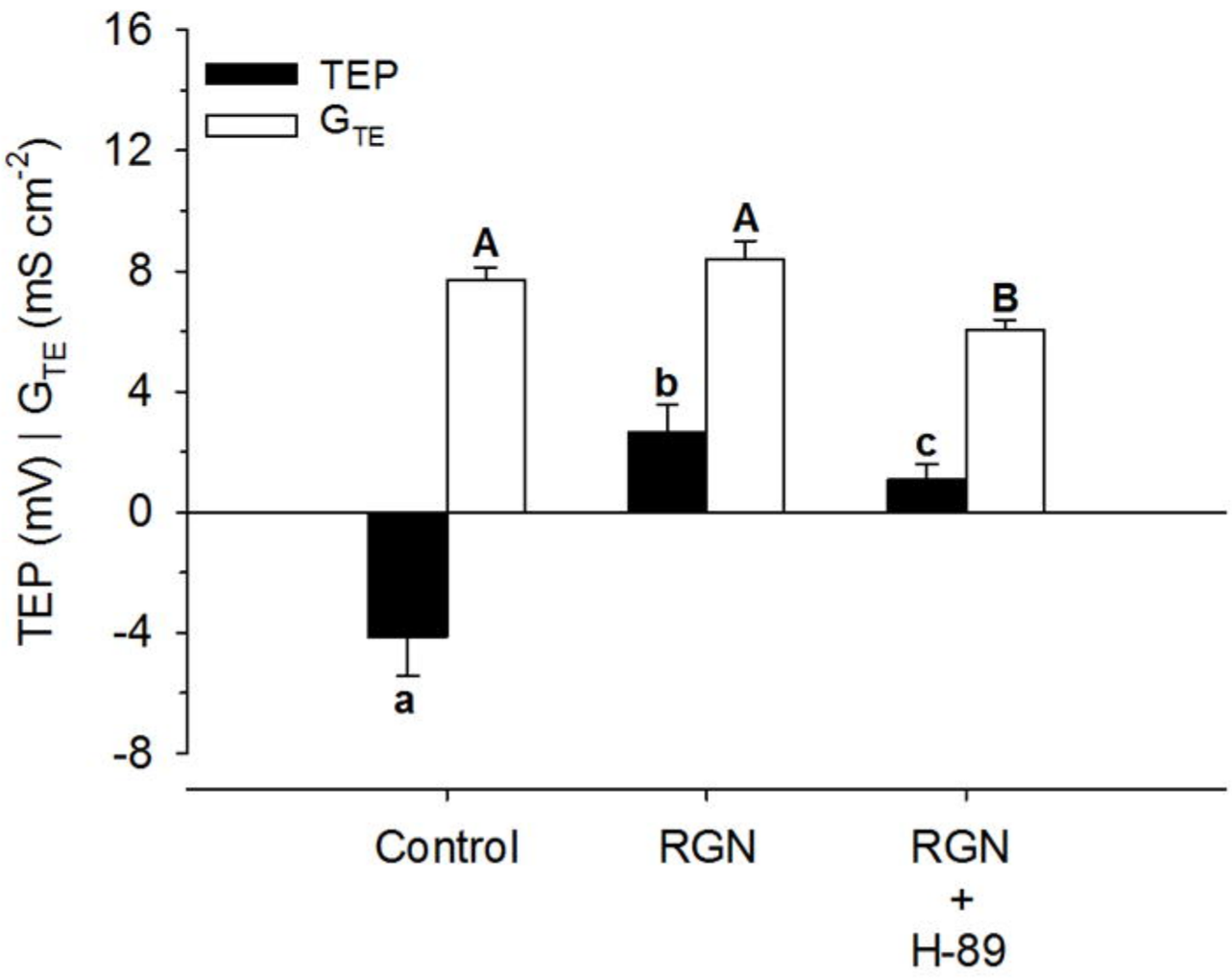
16
12
8
4
0
-4
-8
TEP (mV) | G_{TE} (mS cm^{-2})
TEP
G_{TE}
a
A
b
A
c
B
Control
RGN
RGN + H-89

D

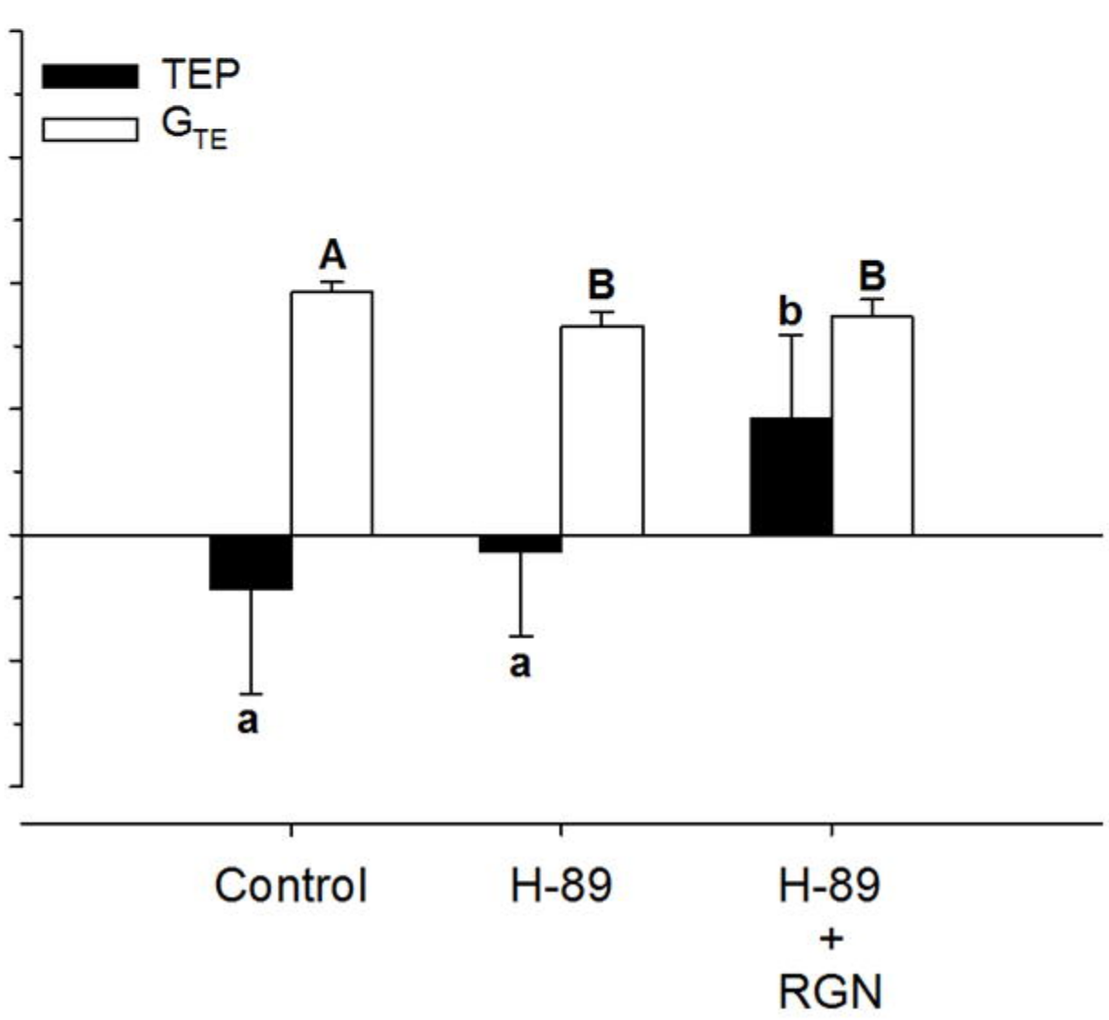
TEP
G_{TE}
a
A
a
B
b
B
Control
H-89
H-89 + RGN

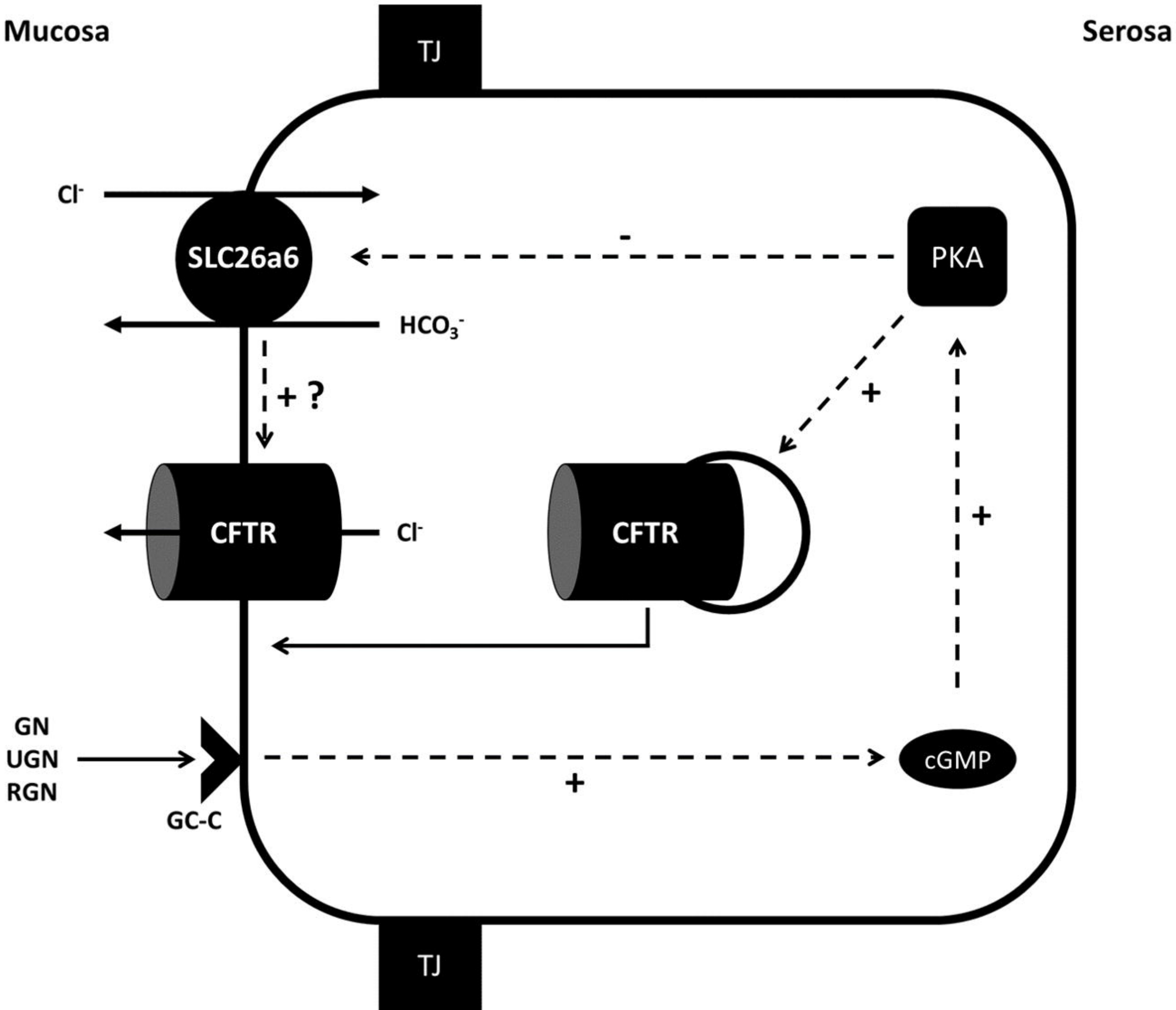
Mucosa
Serosa
TJ
Cl-
SLC26a6
-
PKA
HCO3-
+ ?
+
+
CFTR
Cl-
CFTR
GN
UGN
RGN
GC-C
+
cGMP
TJ